

# Maternal diet–induced microRNAs and mTOR underlie $\beta$ cell dysfunction in offspring

Emilyn U. Alejandro,<sup>1</sup> Brigid Gregg,<sup>2</sup> Taylor Wallen,<sup>1</sup> Doga Kumusoglu,<sup>1</sup> Daniel Meister,<sup>1</sup> Angela Chen,<sup>1</sup> Matthew J. Merrins,<sup>3</sup> Leslie S. Satin,<sup>3</sup> Ming Liu,<sup>1</sup> Peter Arvan,<sup>1</sup> and Ernesto Bernal-Mizrachi<sup>1,4</sup>

<sup>1</sup>Department of Internal Medicine, Division of Metabolism, Endocrinology and Diabetes, Brehm Center for Diabetes Research, <sup>2</sup>Department of Pediatrics, and <sup>3</sup>Department of Pharmacology, University of Michigan, Ann Arbor, Michigan, USA. <sup>4</sup>VA Ann Arbor Healthcare System, Ann Arbor, Michigan, USA.

**A maternal diet that is low in protein increases the susceptibility of offspring to type 2 diabetes by inducing long-term alterations in  $\beta$  cell mass and function. Nutrients and growth factor signaling converge through mTOR, suggesting that this pathway participates in  $\beta$  cell programming during fetal development. Here, we revealed that newborns of dams exposed to low-protein diet (LP0.5) throughout pregnancy exhibited decreased insulin levels, a lower  $\beta$  cell fraction, and reduced mTOR signaling. Adult offspring of LP0.5-exposed mothers exhibited glucose intolerance as a result of an insulin secretory defect and not  $\beta$  cell mass reduction. The  $\beta$  cell insulin secretory defect was distal to glucose-dependent  $\text{Ca}^{2+}$  influx and resulted from reduced proinsulin biosynthesis and insulin content. Islets from offspring of LP0.5-fed dams exhibited reduced mTOR and increased expression of a subset of microRNAs, and blockade of microRNA-199a-3p and -342 in these islets restored mTOR and insulin secretion to normal. Finally, transient  $\beta$  cell activation of mTORC1 signaling in offspring during the last week of pregnancy of mothers fed a LP0.5 rescued the defect in the neonatal  $\beta$  cell fraction and metabolic abnormalities in the adult. Together, these findings indicate that a maternal low-protein diet alters microRNA and mTOR expression in the offspring, influencing insulin secretion and glucose homeostasis.**

## Introduction

The pervasiveness of type 2 diabetes (T2D) is a major public health concern worldwide. The elevated prevalence of this disease results in part from an increased rate of obesity in individuals with genetic predisposition for T2D. Genetic studies have demonstrated that known variants account for less than 10% of the estimated overall genetic contribution to T2D predisposition, suggesting that additional unidentified factors contribute to susceptibility of this disease (1, 2). The fetal nutrient environment has been proposed as another component that might modify the risk for developing diabetes later in life (3). There is increasing evidence that alterations in fetal nutrients not only affect fetal/infant growth but also promote a “thrifty phenotype” that increases the subsequent risk of metabolic syndrome, obesity, and T2D (4). Indeed, maternal malnutrition during pregnancy is known to predispose offspring to adult-onset metabolic disorders such as T2D (3). Such adverse outcomes point to the importance of optimal nutrition during pregnancy for maintaining the long-term function of key metabolic tissues, such as pancreatic  $\beta$  cells. Animal studies in rodents demonstrate that the protein supply during pregnancy plays a key role in the development of  $\beta$  cells (5–7). Thus, the offspring of rats fed a low-protein diet during gestation, a model of intrauterine growth restriction (IUGR), exhibit reduced neonatal  $\beta$  cell proliferation, islet size, and vasculature (6) as well as impaired glucose tolerance in adulthood (7). Despite a considerable number of

studies focused on this topic, how the fetal nutrient environment induces permanent changes in the structure or function of  $\beta$  cells ( $\beta$  cells programming) remains unclear (8).

Presently, there are few studies defining the molecular mechanisms responsible for  $\beta$  cell programming during development. Available mechanistic studies from islets of various animal models of IUGR suggest that critical transcription factors are permanently modified. For example, maternal protein restriction has been shown to alter the methylation status of the *Hnf4a* promoter (9). Intra-uterine artery ligation, a model of placental insufficiency, leads to changes in both DNA methylation and histone acetylation of the *Pdx1* promoter (10). In addition to these key transcription factors important for  $\beta$  cell development, reduced insulin-like growth factor II has also been implicated as playing a role in the alteration of islet cell replication and survival in low-protein-fed offspring (11). These data suggest that the underlying mechanisms of  $\beta$  cell programming are complex and multifactorial. To date, the signaling events linking nutrient status to these alterations are not completely understood.

Both human IUGR patients and murine models of protein restriction have demonstrated decreased placental leucine transport and reductions in essential amino acids in dams (12, 13). Dietary leucine supplementation attenuates fetal growth restriction due to a low-protein diet in rats (14). We postulated that protein restriction in dams results in reduced fetal amino acid levels in the fetuses, which may contribute to altered metabolic programming of developing  $\beta$  cells. The mechanistic target of rapamycin (mTOR) signaling pathway is one of the main mediators of the cellular response to changes in nutrients, including amino acids. mTOR exists in 2 multiprotein complexes

**Conflict of interest:** The authors have declared that no conflict of interest exists.

**Submitted:** November 12, 2013; **Accepted:** July 24, 2014.

**Reference information:** *J Clin Invest*. 2014;124(10):4395–4410. doi:10.1172/JCI74237.

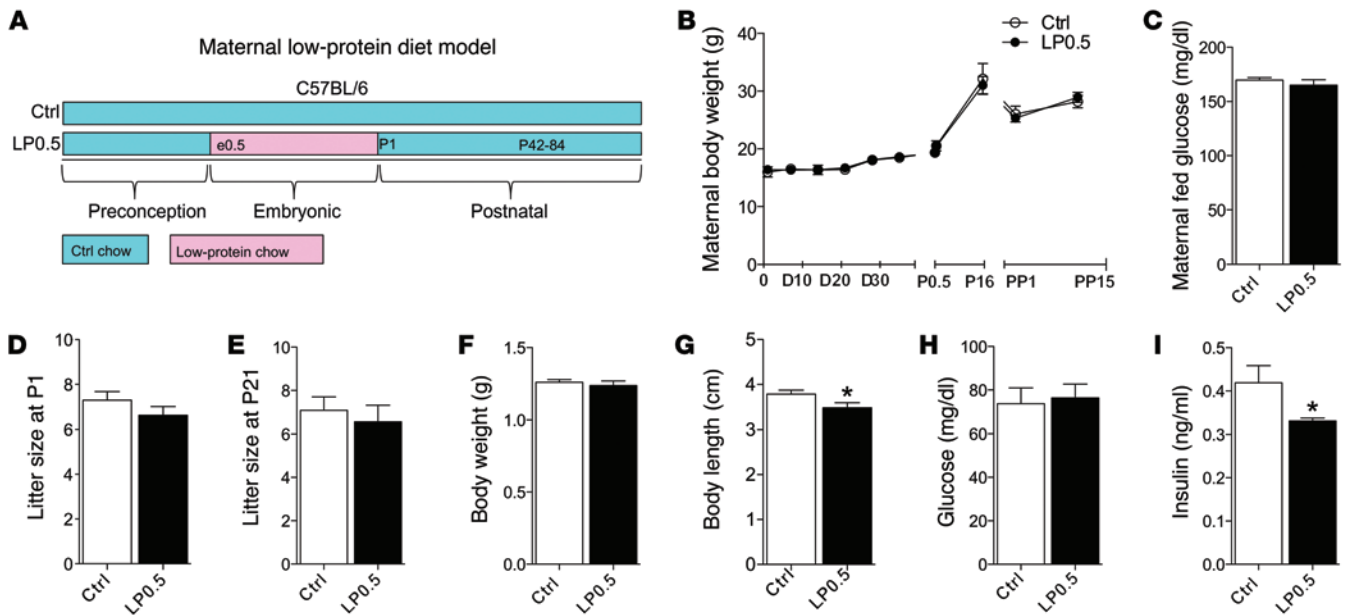


**Figure 1. Maternal low-protein diet model and phenotypes of newborn offspring.** (A) Pregnant C57BL/6 mice were exposed to diets, Ctrl (23% protein) or LPO.5 (isocaloric and 9% protein), throughout pregnancy. After delivery, LPO.5 and Ctrl dams and offspring were introduced to Ctrl. Pancreata were collected at birth and on P84. Metabolic studies of male and female LPO.5 and Ctrl offspring were conducted between day 42 and 84. (B) Maternal body weight during the adaptation period (D0–D30), during pregnancy (P.05–P16), and after pregnancy (PP1–PP15). (C) Maternal fed glucose levels of LPO.5 and Ctrl dams on pregnancy day 15. (D and E) Litter size on P1 (D) and P21 (E). (F and G) Newborn body weight (F) and body length (G). (H and I) Newborn blood glucose (H) and insulin (I) levels in LPO.5 and Ctrl offspring.  $n = 4$  dams were used for maternal body weight assessment (B and C).  $n = 16$ –27 mice were used for D–F.  $n = 8$  mice were used for G–I. \* $P < 0.05$  vs. Ctrl.

that have distinct biological functions (mTORC1 and mTORC2) and couples signals from amino acids and growth factors to the regulation of cell cycle progression, cell fate, and cell growth. mTOR signaling has been shown to regulate  $\beta$  cell mass and function (15–18) as well as  $\beta$  cell development (19). However, the mechanisms by which the nutrient environment during fetal life modulates mTOR signaling and  $\beta$  cell development to alter the susceptibility to diabetes are unknown.

In the present study, we used a maternal low-protein murine model to delineate the mechanisms that regulate programming of neonatal  $\beta$  cell fraction and function and subsequent diabetes susceptibility in adult life. First, we demonstrated that offspring of low-protein diet-fed (LPO.5-fed) dams have reduced mTOR signaling that was associated with reduced neonatal  $\beta$  cell fraction and insulin levels. Adult offspring of dams fed LPO.5 (referred to as LPO.5 offspring) exhibited impaired glucose tolerance due to  $\beta$  cell dysfunction and not to a defect in  $\beta$  cell mass. These alterations in insulin secretion resulted in part from a reduction in mTOR protein levels as a result of enhanced expression of specific microRNAs (miRs) in LPO.5 islets. Inhibition of these miRs in turn normalized both mTOR protein levels and insulin dysfunction in the islets of low-protein-fed offspring. Finally, we used genetically modified mice to rescue the neonatal  $\beta$  cell fraction and metabolic phenotype of low-protein-fed offspring by increasing mTORC1 function only during development. Mice overexpressing Rheb protein, an established positive regulator of mTORC1 signaling, during the last week of gestation ameliorated the glucose intolerance and impaired insulin secretion of adult mice exposed to maternal low-protein diet. These

data indicate that mTORC1 signaling is essential for attenuating  $\beta$  cell dysfunction induced by maternal low-protein diet.

## Results

*Newborns of dams fed LPO.5 have normal body weight but reduced insulin levels.* To elucidate the mechanisms underlying the phenotype of maternal low-protein offspring, we developed a murine model of maternal low-protein exposure using the C57BL/6 strain, as illustrated in Figure 1A. Dams fed control diet (Ctrl) and low-protein diet (LPO.5) throughout pregnancy had similar body weights during the adaptation period (days 0–30) and similar weight gain throughout pregnancy (days 0.5–16 of pregnancy) and after pregnancy (days 1–15 after pregnancy, Figure 1B). LPO.5 feeding during pregnancy did not affect maternal random glucose levels, which were assessed during the second week of pregnancy (Figure 1C). No significant differences were found in litter size at birth or at weaning (P1 and P21, Figure 1, D and E). Additionally, the length of gestation was not different between cohorts (data not shown). These results are consistent with a previously described murine model (20). To characterize the phenotype of maternal protein-restricted offspring (LPO.5), we measured body weight and length as well as the blood glucose levels of LPO.5 neonates. No significant differences in body weight were detected between newborns of dams fed LPO.5 (referred to as LPO.5 newborns) and controls (Figure 1F). Interestingly, a significant decrease in body length was detected in LPO.5 newborn offspring compared with that in control newborns (Figure 1G). Although no difference in blood glucose levels was detected, a significant reduction in insulin levels was observed in the LPO.5 newborns (Figure 1, H and I).

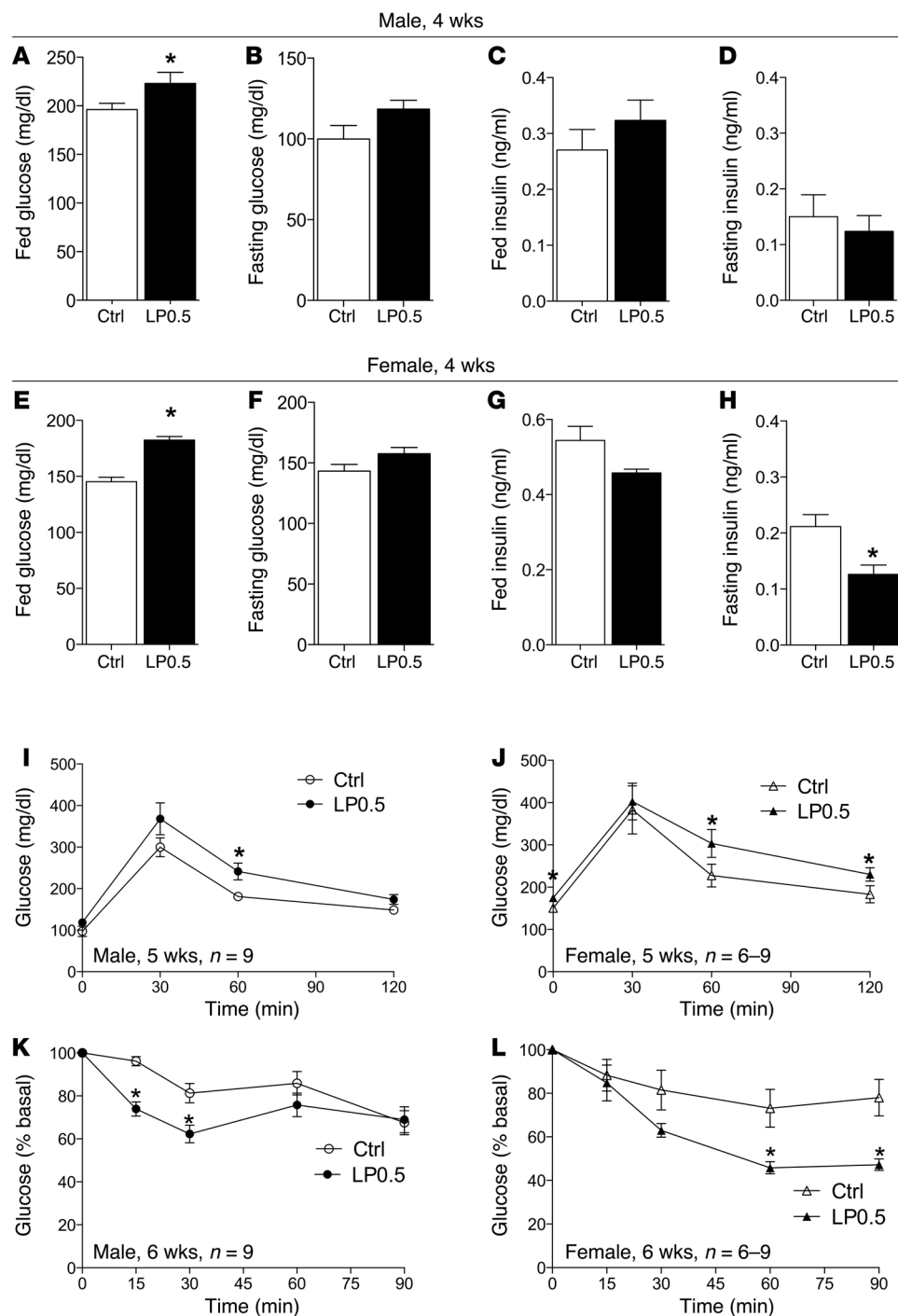


**Figure 2. LPO.5 adult offspring exhibited impaired glucose tolerance and enhanced insulin sensitivity.** (A, B, E, and F) Fed or fasting glucose levels in 4-week-old male (A and B) and female (E and F) LPO.5 and Ctrl mice. (C, D, G, and H) Fed or fasting insulin levels in 4-week-old male (C and D) and female (G and H) LPO.5 and Ctrl mice. (I–L) Intra-peritoneal glucose and insulin tolerance tests were performed in 5- and 6-week-old male (I and K) and female (J and L) LPO.5 and Ctrl mice. \**P* < 0.05 vs. Ctrl. *n* = 5 for both male and female unless otherwise noted.

*LPO.5 adult offspring exhibit impaired glucose tolerance and enhanced insulin sensitivity.* The fed glucose levels of 4-week-old LPO.5 male and female offspring were elevated compared with those of controls (Figure 2, A and E). No differences, however, were detected in the corresponding fed insulin levels of either male or female groups (Figure 2, C and G). In the fasting state, 4-week-old LPO.5 male and female mice exhibited fasting glucose levels comparable to those of the controls (Figure 2, B and F), while a significant reduction in fasting insulin was detected in the LPO.5 female, but not male, mice compared with controls (Figure 2, D and H). To further determine the impact of LPO.5

on glucose homeostasis, we performed glucose tolerance testing. Impaired glucose tolerance was present in 5-week-old male and female LPO.5 mice compared with controls (Figure 2, I and J). The effects of LPO.5 on glucose tolerance coupled with the reduced fasting insulin levels seen in the female mice suggest that LPO.5 mice were more insulin sensitive than controls. Indeed, insulin tolerance tests revealed that male and female LPO.5 mice were more insulin sensitive than control mice (Figure 2, K and L). Thus, these studies demonstrated that low-protein diet during pregnancy resulted in impaired glucose tolerance and enhanced insulin sensitivity in 6-week-old offspring.

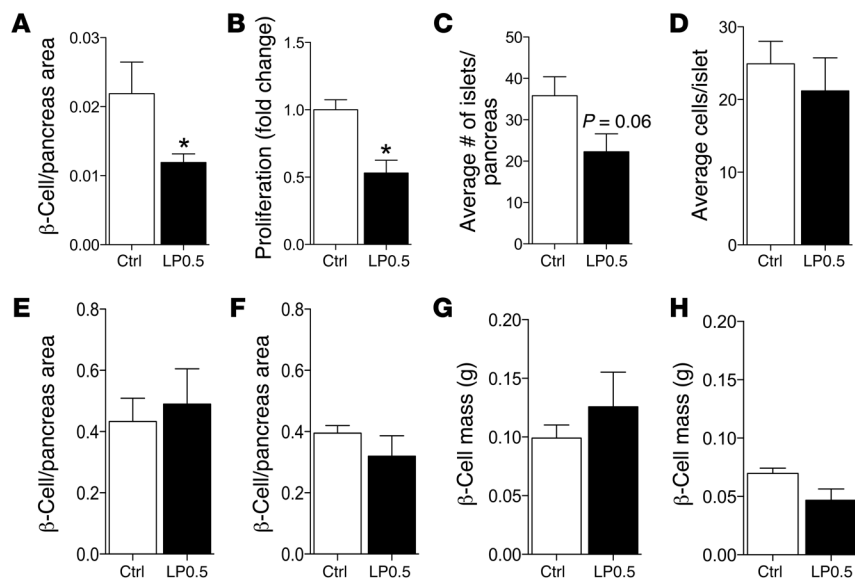


**Figure 3. LPO.5 offspring exhibit abnormal neonatal  $\beta$  cell fraction.** (A)  $\beta$  Cell/pancreas area in newborn LPO.5 and Ctrl mice. (B)  $\beta$  Cell proliferation, as measured by Ki67 staining, in newborn LPO.5 and Ctrl mice. (C) Average number of islets per pancreas in LPO.5 and Ctrl mice at birth. (D) Average  $\beta$  cell number per islet in LPO.5 and Ctrl mice at birth. (E and F) Normalized  $\beta$  cell/pancreas area in 3-month-old male (E) or female (F) LPO.5 and Ctrl mice. (G and H)  $\beta$  Cell mass in 3-month-old male (G) or female (H) LPO.5 and Ctrl mice. \* $P < 0.05$  vs. Ctrl,  $n \geq 5$ .

*LPO.5 offspring exhibit abnormal neonatal  $\beta$  cell fraction.* The combination of glucose intolerance, despite increased insulin sensitivity, in LPO.5 mice suggested a defect in functional pancreatic  $\beta$  cell mass. To determine the impact of LPO.5 on  $\beta$  cell development and mass, we assessed  $\beta$  cell morphology at different stages. To determine abnormalities in the  $\beta$  cell/pancreas ratio, we examined pancreata from newborn LPO.5 mice. Due to the inherent inaccuracy in measuring pancreatic weight in neonates, we measured  $\beta$  cell/pancreas area ratio and not  $\beta$  cell mass. LPO.5 newborns had a significant reduction in  $\beta$  cell/pancreas ratio (fraction) and  $\beta$  cell proliferation, as measured by Ki67 staining (Figure 3, A and B). Although it was not significant, there was a trend toward an alteration in the average number of islets per pancreas section (Figure 3C). No differences in the average  $\beta$  cell number per islets were observed (Figure 3D). Alterations in neonatal  $\beta$  cell/pancreatic ratio were not observed in 3-month-old male and female LPO.5 mice compared with controls (Figure 3, E and F). When accounting for pancreas weight, no significant differences were found in  $\beta$  cell mass in adult male or female LPO.5 mice (Figure 3, G and H). These data indicate that exposure to LPO.5 during development alters endocrine cell development, resulting in abnormalities in the neonatal  $\beta$  cell/pancreas ratio that appear to recover after adequate postnatal nutrition is supplied.

*LPO.5 adult offspring have an insulin secretion defect that is distal to  $Ca^{2+}$  signaling.* The abnormalities in glucose tolerance in the presence of enhanced insulin sensitivity and  $\beta$  cell mass in 12-week-old LPO.5 offspring suggested that stimulus-secretion coupling or insulin biosynthesis could be perturbed (Figure 4, A and B). The capacity of  $\beta$  cells to secrete insulin in response to glucose in vivo was blunted in 3-month-old LPO.5 mice compared with that in controls (Figure 4C). To corroborate these in vivo findings, and to remove the possible influence of hormonal and neuronal stimuli, the glucose dependence of intracellular  $Ca^{2+}$  and insulin secretion was next assessed in isolated LPO.5 islets in vitro. Glucose-induced insulin secretion in LPO.5 islets was reduced despite having less insulin content (Figure 4, D and E). Therefore, the defect in insulin secretion results from a combination

of an insulin secretory defect and a reduction in insulin content. In addition, KCl-induced insulin secretion was also significantly reduced (Figure 4F). This secretory defect in LPO.5 islets was not due to alterations in the frequency or amplitude of glucose-stimulated intracellular  $Ca^{2+}$  oscillations (Figure 4, G–J). Taken together, these data demonstrate that the nutritional insult experienced during development induced long-lasting defects in stimulus-secretion coupling. These consequences appeared to occur distal to  $Ca^{2+}$  entry at the level of either the exocytosis machinery or in insulin biosynthesis.

*LPO.5 exposure during pregnancy alters *Ins2* and *Pdx1* mRNA and  $\beta$  cell insulin content in adult mice.* We hypothesized that reduced insulin content could also play a role in the abnormalities we observed in insulin secretion. A reduction in insulin content was observed in both male and female islets isolated from the LPO.5 mice (Figure 5, A and B). To determine the mechanisms underlying this, the transcript levels of the insulin 1 and 2 genes (*Ins1* and *Ins2*) were measured by quantitative real-time PCR. Indeed, an approximately 50% reduction in *Ins2* mRNA was evident, with no change in *Ins1* levels, in LPO.5 islets compared with controls (Figure 5, C and D). This *Ins2* mRNA change was associated with decreased proinsulin biosynthesis in LPO.5 islets after a 10-minute pulse labeling (Supplemental Figure 2, A–C; supplemental material available online with this article; doi:10.1172/JCI74237DS1). However, no changes in insulin processing were observed (Supplemental Figure 2D). Next, we examined the gene expression of transcription factors that are known to modulate insulin biosynthesis, and we observed a significant reduction in *Pdx1* mRNA in the islets of LPO.5 mice compared with that in controls (Figure 5E). These changes in *Pdx1* were accompanied by reduced *Pdx1* protein, which may partially explain the reduced level of insulin content in the LPO.5 mice (Figure 5, F and G). *Mafa* mRNA expression and protein levels were not altered in LPO.5 islets compared with controls (Supplemental Figure 1, A–C). Interestingly, no changes in *Neurod1*, *Hnf1a*, *Hnf4a*, *Tcf2*, *Igf2*, and glucokinase (*Glc*) mRNA were observed in LPO.5 islets (Figure 5, H–M). Transcriptional regulation of *Ins1* has been shown to be selectively controlled by

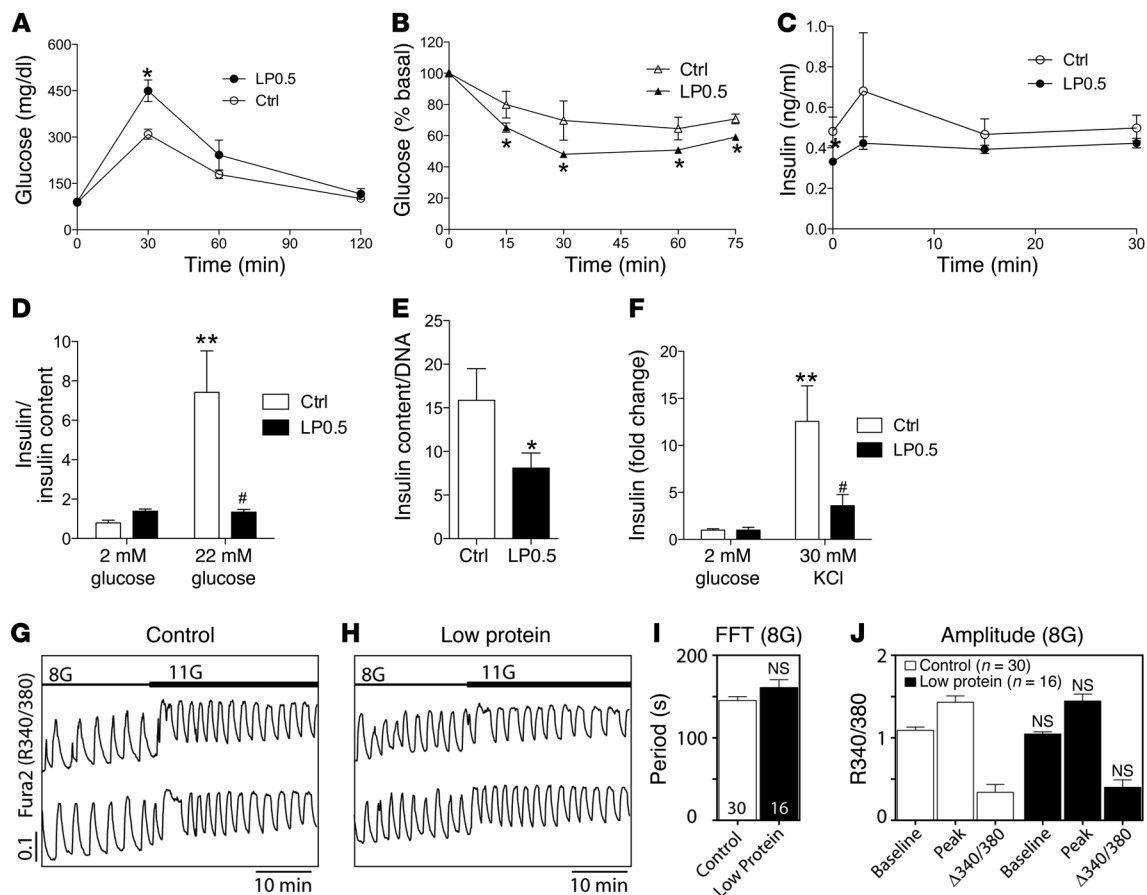


**Figure 4. LP0.5 adult offspring have insulin secretion defect that is distal to calcium signaling.** (A and B) Intraperitoneal glucose tests (A) and insulin tolerance tests (B) in 12-week-old male LP0.5 and Ctrl mice. (C) In vivo glucose-stimulated insulin secretion in 12-week-old male LP0.5 and Ctrl mice. (D) Glucose-stimulated insulin secretion in isolated islets from adult LP0.5 and Ctrl mice in response to 2 mM and 16 mM glucose. Secreted insulin was normalized to total content. (E) Total islet insulin content in D was measured and normalized to total islet DNA. (F) Insulin secretion in response to 30 mM KCl. (G and H) Representative recordings of intracellular calcium are shown in islets isolated from Ctrl or LP0.5 mice stimulated with 8 mM (8G) and 11 mM glucose (11G). (I) Average oscillatory period was determined by fast Fourier transform (FFT) from >20 minutes of recording. Numbers on bars indicate number of islets measured in  $\geq 4$  independent experiments from 2 cohorts. (J) Average oscillatory baseline, peak, and amplitude ( $\Delta 340/380$ ) are displayed as in I. No significant differences were found. \* $P < 0.05$  vs. Ctrl, \*\* $P < 0.05$  vs. Ctrl 2 mM glucose, # $P < 0.05$  vs. Ctrl 22 mM glucose.

NeuroD1 in adult  $\beta$  cells (21), which may explain why *Ins1* mRNA levels were unaltered in the LP0.5 mice. Taken collectively, the data suggest that glucose intolerance in LP0.5 offspring is caused, at least in part, by defective insulin secretion and reduced insulin content. The reduction in insulin content results from decreased proinsulin biosynthesis secondary to alterations in *Pdx1* levels and *Ins2* gene transcription.

*LPO.5 exposure during pregnancy decreases mTOR signaling in neonatal and adult  $\beta$  cells.* To determine the effects of maternal low-protein diet on mTORC1 signaling, we performed immunostaining for phosphorylated ribosomal protein S6 at Ser240 and insulin in newborn islets. We observed a reduction in phosphorylated S6 at Ser240 in LP0.5 newborn  $\beta$  cells (Figure 6A), suggesting that LP0.5 exposure reduced mTORC1 activity in  $\beta$  cells at birth. Next, we determined the extent to which the alterations in mTOR signaling that we observed in LP0.5 neonates persisted in LP0.5 adults. Indeed, total mTOR protein levels were reduced in the islets of 3-month-old LP0.5 females and males compared with those in controls (Figure 6, B-E). However, this decrease in mTOR expression was not asso-

ciated with alterations in global protein synthesis in LP0.5 islets (Supplemental Figure 2E). As expected, the reduction in mTOR protein levels was also associated with decreased phosphorylation of ribosomal protein S6 at Ser240 in adult LP0.5 islets, suggesting that mTOR complex 1 (mTORC1) activity was decreased (Figure 6, F and G). Nonendocrine pancreas lysates showed increased mTOR levels, while liver lysates had normal mTOR levels (Supplemental Figure 1, C-G). A trend toward decreased phosphorylation of ERK1/2 in LP0.5 islets lysates was also observed (Figure 6, F and H), which may independently contribute to the reduced insulin transcription we saw in LP0.5 mice. Phosphorylation of AKT at Ser473, a known target of mTORC2, was also altered in islets taken from LP0.5 mice (Figure 6, F and I). Together, these data suggest that LP0.5 mice have a sustained downregulation of mTOR protein, resulting a decrease in the activity of mTORC1 and mTORC2 in the adult offspring of dams fed a low-protein diet.

*LPO.5 exposure during pregnancy regulates mTOR signaling in adult mice by altering specific miRs.* To elucidate the mechanisms underlying the reduction of mTOR protein we observed,

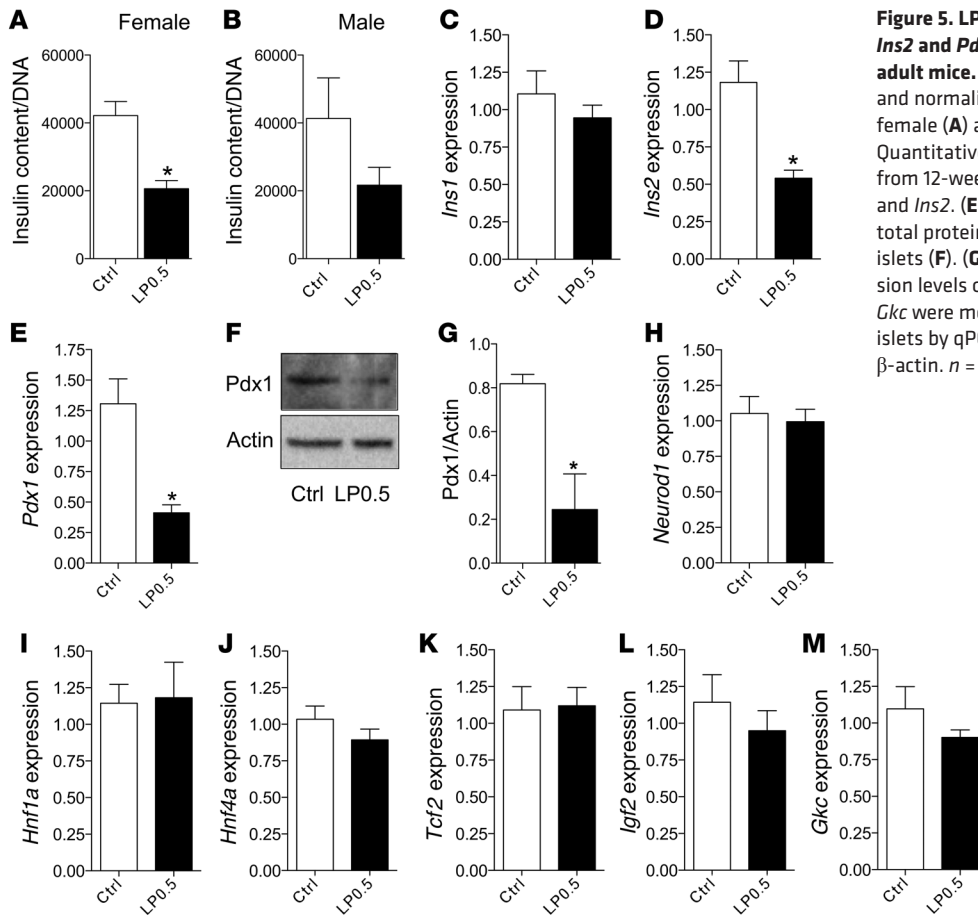


**Figure 5. LPO.5 exposure during pregnancy alters *Ins2* and *Pdx1* mRNA and  $\beta$  cell insulin content in adult mice.** (A and B) Insulin content was determined and normalized to total islet DNA in 12-week-old female (A) and male (B) LPO.5 and Ctrl mice. (C and D) Quantitative PCR was performed on isolated mRNA from 12-week-old male LPO.5 and Ctrl islets for *Ins1* and *Ins2*. (E and F) *Pdx1* mRNA expression (E) and total protein levels from 12-week-old LPO.5 and Ctrl islets (F). (G) Quantification of F. (H–M) mRNA expression levels of *Neurod1*, *Hnf1a*, *Hnf4a*, *Tcf2*, *Igf2*, and *Glc* were measured in male 12-week-old LPO.5 and Ctrl islets by qPCR. Transcript levels were normalized to  $\beta$ -actin.  $n = 4$ –6 for C–M. \* $P < 0.05$  vs. Ctrl,  $n \geq 3$ .

we assessed *mTOR* mRNA levels, and no significant changes in *mTOR* transcript expression were observed, suggesting that the defect in *mTOR* protein levels in LPO.5 is posttranscriptional (Figure 7A). Because miRNAs play an important role in regulating key genes at the posttranscriptional level, we investigated the role of miRNAs on regulation of *mTOR* in 3-month-old LPO.5 mice. To identify miRNAs differentially expressed in islets of LPO.5 offspring, we pursued (a) a candidate-based screen for miRNAs that regulate *mTOR* and (b) an unbiased approach using a PCR-based array. miR-7, -99, and -199a-3p have previously been demonstrated to regulate *mTOR* signaling or *mTOR* protein directly in multiple tissues (22–25). Assessment of these miRNAs revealed that miR-7 and -199a-3p were significantly increased in adult LPO.5 islets compared with controls (Figure 7, B and D). However, no changes in miR-99 were observed in LPO.5 islets compared with controls (Figure 7C). Next, we analyzed 720 miRNAs in islets from LPO.5 and control mice using a real-time PCR-based microarray (OpenArray microarray) in order to discover novel miRNAs that might drive the  $\beta$  cell programming effect we observed in LPO.5 offspring. Among the 720 miRNAs we measured, approximately 537 showed readable values in islets. Of these, only 14 were significantly altered; 2 were increased (Table 1), and 12 were reduced (Table 2). miR-152 and -342 were increased in the microarray. miR-7 and -199a-3p, which were selected from the candidate approach, were increased in the microarray but did not reach significance (with fold changes of 1.91 and 2.36, respectively). Although expression of miR-7a has

previously been reported in islets, expression of miR-152, -199a-3p, and -342 in islets is presented here for the first time. One common target of miR-7, -199a-3p, and -152 is *mTOR* signaling (22, 24, 26). However, computational predictions using miRGen Targets (27) (intersection of PicTar and TargetScanS prediction programs) indicate that miR-152 and -342 may also target multiple proteins regulating transport, GTPase activators, and actin polymerization and binding, the combined effect of which may play a role in insulin secretion.

*miR-199a-3p and -342 regulate mTOR protein levels and insulin secretion in  $\beta$  cells.* To delineate the mechanisms responsible for *mTOR* reduction and insulin secretory dysfunction in islets of LPO.5 offspring, we carried out further investigations of the effects of miR-199a-3p and -342. We focused on miR-199a-3p, because it has recently been shown to directly bind to the *mTOR* 3' UTR and affect *mTOR* protein levels but not mRNA expression (24). To test whether miR-199a-3p could regulate the expression of endogenous *mTOR*, a miR-199a-3p inhibitor (anti-miR-199a-3p) was transfected into dispersed islet cells isolated from adult LPO.5 and control offspring. Thirty-six hours after transfection, anti-miR-199a-3p was found to normalize *mTOR* and *Pdx1* protein levels in LPO.5 islets to control levels (Figure 8, A and B). A nonsignificant increase in *mTOR* protein levels in control cells transfected with anti-miR-199a-3p ( $P = 0.07$ ) was also observed. Blocking miR-199a-3p in dispersed human islet cells also increased *mTOR* protein levels (Supplemental Figure 3, A and B). Subsequently,

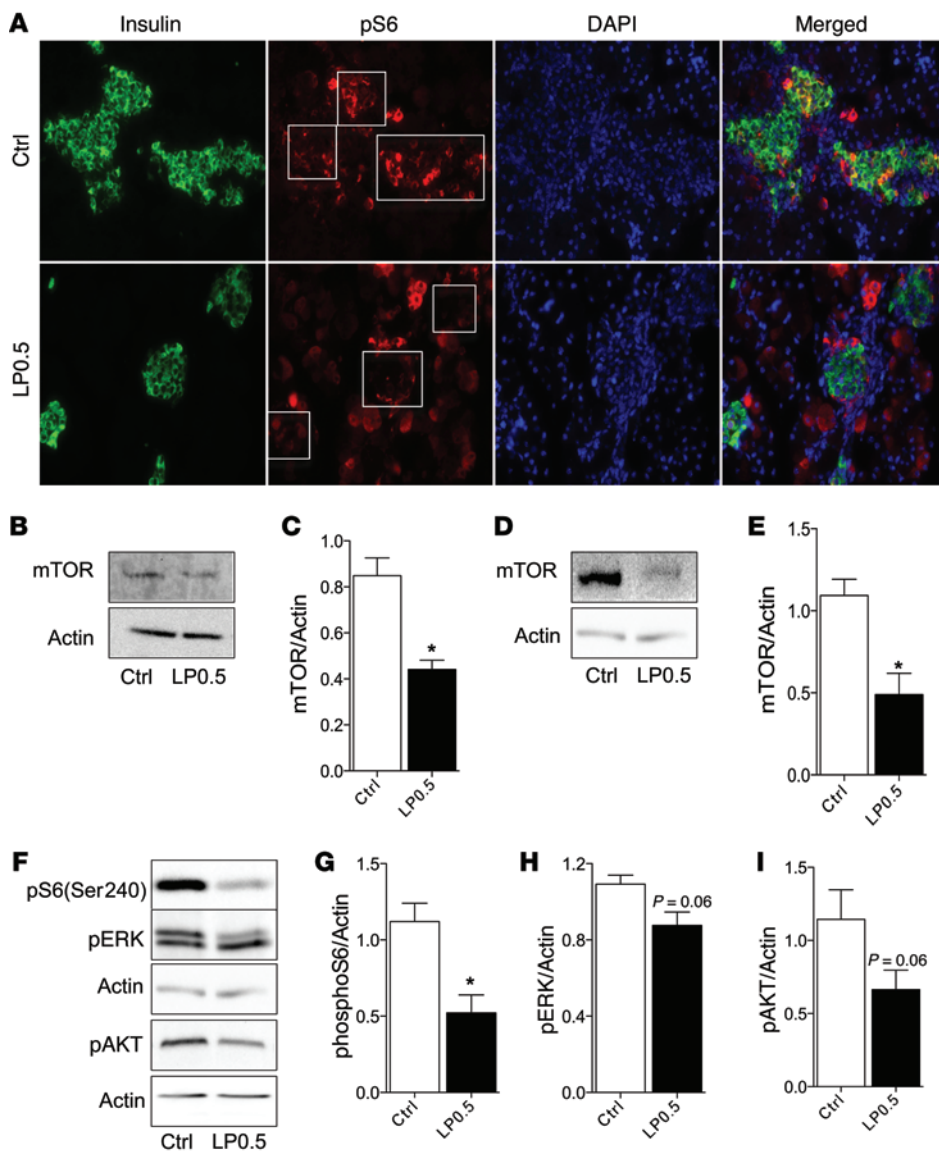


**Figure 6. LP0.5 exposure during pregnancy decreases mTOR signaling in neonatal and adult  $\beta$  cells.** (A) Immunofluorescence staining of phosphorylated ribosomal protein S6 (pS6, Ser240, red) and insulin (green) in neonatal islets (original magnification,  $\times 40$ ) from LP0.5 and Ctrl mice. (B–E) mTOR protein levels in 12-week-old islets from LP0.5 and Ctrl mice. A representative Western blot of mTOR in male (B) and female (D) mice. Quantification of mTOR levels normalized to  $\beta$ -actin in male LP0.5 islets (C) and female LP0.5 islets (E). (F) Phosphorylated ribosomal protein S6, ERK1/2, and AKT1/2 levels in 12-week-old islets from LP0.5 and Ctrl mice. (G–I) Quantification of blots in F. D (mTOR and actin) and F (pS6 Ser240 and actin) are from the same experiment. \* $P < 0.05$  vs. Ctrl,  $n \geq 4$ .

we focused on assessing the effects of miR-342, the most highly induced miR in LP0.5 islets. Interestingly, anti-miR-342 normalized mTOR protein levels in LP0.5 adult islets compared with controls (Figure 8C). Thus, these data suggest that multiple miRs regulate mTOR protein posttranscriptionally in LP0.5 islets.

Next, we assessed whether the normalization of mTOR protein levels in LP0.5 islets could rescue the insulin secretion dysfunction in LP0.5 islets. Anti-miR-199a-3p and -342 were transfected into dispersed islet cells from control or LP0.5 mice, and the glucose-stimulated insulin secretion of these cells was tested. As a positive control, we used a miR-375 inhibitor (anti-miR-375), a well-characterized miR known to block insulin secretion in  $\beta$  cells (28). We observed a significant increase in glucose-stimulated insulin secretion in dispersed  $\beta$  cells from Ctrl-fed mice transfected with anti-miR-375 and -342 compared with scrambled control miR-transfected cells (Figure 8D). As shown previously with intact islets, we observed a significant reduction in glucose-stimulated insulin secretion in the dispersed islet cells from adult LP0.5 mice compared with controls (Figure 8D). As such, along with the nor-

malization of mTOR protein levels in LP0.5 islets, we observed significantly improved insulin secretion in LP0.5 islet cells transfected with anti-miR-199a-3p or -342 (Figure 8D). These data suggest that blocking the effect of miR-199a-3p or -342 is sufficient to rescue defective insulin secretion in islets of LP0.5 mice. Our data also demonstrated that anti-miR-375 was sufficient to rescue the insulin secretion defect in LP0.5 islets (Figure 8D). Anti-miR-199a-3p, -342, or -375 did not affect insulin content in the  $\beta$  cells of control offspring (Figure 8E). However, blocking these miRs normalized insulin content in the LP0.5  $\beta$  cells to control levels (Figure 8E). To further investigate the effects of miR-152 and -342 on insulin secretion, we transfected islet cells from control offspring with miR mimics. Transfection of control islet cells with mimics of miR-152 or -342 reduced the level of insulin secreted in response to glucose without altering insulin content (Figure 8, F and G), suggesting that miR-152 and -342 play an important role in regulating insulin secretion.

*Transient activation of mTORC1 in  $\beta$  cells rescues  $\beta$  cell fraction defect in LP0.5 newborns.* Because mTOR protein level was reduced in LP0.5 islets, we aimed to determine the direct contribution of

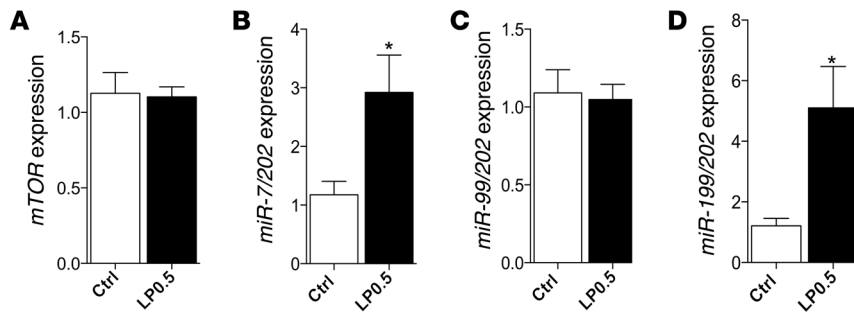


**Figure 7. LP0.5 exposure during pregnancy regulates mTOR signaling in adult mice by altering specific miRs.** (A) *mTOR* transcription message from islets of 12-week-old male LP0.5 and Ctrl mice. (B–D) miRs differentially expressed in islets of 12-week-old male LP0.5 and Ctrl mice. Expression of the indicated miRs was measured by qRT-PCR. Small enriched RNA was purified by using MirVana. Results are expressed as fold changes and correspond to the mean  $\pm$  SEM of LP0.5 and Ctrl mice ( $n = 4$ ). \* $P < 0.05$  vs. Ctrl.

mTORC1 signaling to the  $\beta$  cell programming phenotype induced by LP0.5. To do this, we transiently induced mTORC1 signaling in  $\beta$  cells by conditionally deleting *TSC2*, a negative regulator of mTORC1 signaling, in  $\beta$  cells of LP0.5 offspring from embryonic day 14.5 to birth. Using an additional model, we overexpressed *Rheb*, a positive regulator of mTORC1, from embryonic day 14.5 to birth. Evaluation of newborn body weight and length showed that *Tsc2*-deficient (*RIPCre Tsc2<sup>fl/fl</sup>*) mice and *Tsc2<sup>fl/fl</sup>* littermates (hereafter referred to as wild type) exposed to either Ctrl or LP0.5 during gestation were comparable (Supplemental Figure 4, A and B). We observed similar body weight and length data in *Rheb*-overexpressing (*RIPCre Rheb*) and *Rheb* non-overexpressing (*Rheb* or *RIPCre* wild-type mice) mice exposed to either Ctrl or LP0.5 (Supplemental Figure 4, C and D). Next, we assessed whether the neonatal  $\beta$  cell fraction defect that we observed in C57BL/6 LP0.5 offspring was rescued by the gain of mTORC1 function seen in *RIPCre Tsc2<sup>fl/fl</sup>* or *RIPCre Rheb* mice. Similar to the C57BL/6 strain model, we observed a significant reduction in the  $\beta$  cell/pancreas area in wild-type LP0.5 newborns (Figure 9A) compared with wild-type Ctrl-fed newborn mice (Figure 9A). In contrast, LP0.5 mice with *Tsc2* deletion in  $\beta$  cells (Figure 9A) demonstrated improved neonatal  $\beta$  cell/pancreas area compared with that of wild-type LP0.5 mice (Figure 9A). Next, we assessed the effect of overexpressing *Rheb* in  $\beta$  cells on the neonatal  $\beta$  cell/pancreas area. *RIPCre Rheb* and wild-type (*RIPCre*) newborns exposed to Ctrl during gestation had comparable  $\beta$  cell/pancreas area (Figure 9B). However, the overexpression of *Rheb* in  $\beta$  cells rescued the neonatal  $\beta$  cell/pancreas area defect seen in LP0.5 mice. As expected, LP0.5 wild-type offspring (Figure 9B) had a significant reduction in neonatal  $\beta$  cell/pancreas area compared with that of controls (Figure 9B). On the other hand, *Rheb*-induced enhancement of mTORC1 signaling improved  $\beta$  cell/pancreas area of the LP0.5 offspring (Figure 9B).  $\beta$  Cell proliferation, as measured by Ki67<sup>+</sup> staining (Supplemental Figure 5A), was reduced in wild-type LP0.5 offspring (Figure 9, C and D) compared with that in wild-type Ctrl-fed offspring (Figure 9, C and D). However,  $\beta$  cell proliferation was normalized in LP0.5 *RIPCre Tsc2<sup>fl/fl</sup>* or *RIPCre Rheb* mice compared with that in wild-type offspring (Figure 9, C and D). Therefore, the rescued  $\beta$  cell mass in *RIPCre Tsc2<sup>fl/fl</sup>* and *RIPCre Rheb* mice could be explained, at least in part, by enhanced  $\beta$  cell proliferation.

*Transient activation of mTORC1 in  $\beta$  cells during development rescues glucose intolerance and insulin secretion dysfunction in LP0.5 mice.* To identify the effects of gain of mTORC1 function during the developmental period on the susceptibility to diabetes induced by maternal protein restriction, we transiently induced mTORC1 signaling from embryonic day 14.5 to birth

and then assessed glucose tolerance and insulin secretion in adult animals. To study adult mice, we used a model having conditional and inducible *Rheb* overexpression in  $\beta$  cells. This model allowed us to study the effect of *Rheb* activation exclusively during a specific window of development on glucose homeostasis later in adult mice. By taking advantage of the Tet-Off binary transgenic system, the expression of the *Rheb* transgene was dependent on the activity of tTA, such that the activation of mTORC1 signaling could be turned off by administering doxycycline (Dox) in the diet. An internal ribosome entry site in the construct allowed the coupled expression of EGFP for lineage tracing. Therefore, LP0.5 progeny with a genotype of *RIPCre Rheb* will have a transient activation of mTORC1 signaling only from E14.5 to just a few days after birth. Recombination efficiency and *Rheb* signaling activation were assessed by EGFP expression. EGFP immunofluorescence was visible only in  $\beta$  cells of *RIPCre Rheb* newborn mice compared with that in wild-type (*RIPCre* or *Rheb*) newborn mice (Supplemental Figure 6A). EGFP was not detectable in adult *RIPCre Rheb* mice exposed to Dox throughout life (Supplemental Figure 6, B and C). To metabolically characterize *RIPCre Rheb* mice, we performed glucose tolerance tests in 3-month-old *RIPCre Rheb* and *RIPCre* mice not exposed to Dox treatment. Interestingly, glucose tolerance was comparable between *RIPCre Rheb* mice and control (*RIPCre*) mice (Figure 9E). Glucose-stimulated insulin secretion in these mice was also normal (E.U. Alejandro et al., unpublished observations). Next, we tested whether activating mTORC1 by overexpressing *Rheb* only during the last week of development improved glucose tolerance in adult LP0.5 mice. Consistent with our previous findings, Ctrl-fed wild-type offspring (Ctrl *Rheb* + Dox) showed improved glucose tolerance compared with that of wild-type LP0.5 (LP0.5 *Rheb* + Dox) mice at 3 months of age

**Table 1. Increased miRs in adult islets from LP0.5 mice**

miRs	LogFC	P value
miR-152	0.52375	0.008658009
miR-342-5p	2.384891667	0.017316017

Summary of microarray data comparing adult LP0.5 and Ctrl islets. Only microarray passing the stringent threshold for significant change are shown. Islets were harvested from male 12-week-old LP0.5 and Ctrl mice, and RNA was isolated by the MirVana Kit for OpenArray microarray. Quality of RNA was assessed by an Agilent Bioanalyzer ( $n = 5$ ). Log<sub>2</sub>FC, log<sub>2</sub> fold change.



**Table 2. Reduced miRs in adult islets from LP0.5 mice**

miRs	LogFC	P value
miR-30b	-0.887604167	0.0086580
miR-1903	-9.64619375	0.015873016
miR-697	-6.473	0.015873016
miR-669N	-0.715870833	0.017316017
miR-487b	-0.286583333	0.025974026
miR-27b#	-0.6698375	0.03030303
miR-1954	-1.907504167	0.03030303
miR-671-5P	-2.486604167	0.03030303
miR-1306	-1.455975	0.031746032
miR-101a#	-1.78945	0.035714286
miR-224	-0.540416667	0.041125541
miR-491	-1.180083333	0.041125541

Summary of microarray data comparing adult LP0.5 and Ctrl islets. Only microarray passing the stringent threshold for significant change are shown. Islets were harvested from 12-week-old LP0.5 and Ctrl mice, and RNA was isolated by the MirVana Kit for OpenArray microarray. Quality of RNA was assessed by an Agilent Bioanalyzer ( $n = 5$ ).

(Figure 9F). *RIPCre Rheb* mice (LP0.5 *RIPCre Rheb* + Dox) had significantly improved glucose tolerance compared with that of LP0.5 wild-type (LP0.5 *Rheb* + Dox, Figure 9F). There were no differences in insulin sensitivity between LP0.5 *RIPCre Rheb* and *Rheb* Dox-treated mice (data not shown). Moreover, insulin secretion was enhanced in LP0.5 *RIPCre Rheb* mice compared with that in LP0.5 *Rheb* mice treated with Dox (Figure 9G).

To investigate how *Rheb* overexpression during pregnancy rescues the LP0.5 mouse phenotype, we assessed mTOR protein levels, mTORC1 activity, Pdx1 expression, and miR levels in islets from the different experimental groups. As shown before, mTOR, phosphoS6 levels, and Pdx1 expression were reduced in LP0.5 *Rheb* + Dox mice compared with Ctrl *Rheb* + Dox mice (Figure 9, H–J and N). Remarkably, mTOR levels and activation of mTORC1 signaling, as assessed by phosphorylated S6 levels in islets from LP0.5 *RIPCre Rheb* mice, were restored to the levels observed in Ctrl *RIPCre Rheb* mice (Figure 9, K–M). In addition Pdx1 levels in LP0.5 *RIPCre Rheb* islets were returned to the levels in *RIPCre Rheb* mice exposed to Ctrl (Ctrl *RIPCre Rheb*) (Figure 9, N–Q). In addition, increased *Ins2* mRNA was observed in LP0.5 *RIPCre Rheb* mice compared with that in LP0.5 mice (Supplemental Figure 7A). The beneficial changes obtained by *Rheb* overexpression in LP0.5 mice appeared to be independent of the expression of miR-199a-3p, -152, and -7a (Supplemental Figure 7, B–D). Collectively, these data provide genetic evidence that transient activation of mTORC1 in  $\beta$  cells during last week of pregnancy improves glucose tolerance by enhancing insulin secretion in LP0.5 mice and point to a mechanistic role of mTOR signaling in  $\beta$  cell programming.

## Discussion

It is widely accepted that nutrition during early life affects the development and function of specific organs as well as the overall metabolism of an entire organism many years later in life. Multiple animal models, including maternal protein restriction, caloric restriction, and intrauterine placental ligation models, have

identified common metabolic phenotypes in offspring and have identified the pancreatic  $\beta$  cell as particularly sensitive to nutrients very early in life (3, 29, 30). In these experiments, we used engineered animal models with spatial and temporal regulation capabilities to dissect the molecular mechanisms responsible for developmental programming by low protein. In the present study, maternal low-protein diet induces permanent changes in  $\beta$  cell function of LP0.5 offspring by altering miR expression, mTOR protein levels, and Pdx1 and insulin mRNA and protein levels. These studies also demonstrate that mTOR, a major target of nutrients and growth factors, is modulating the effects of nutrient programming of metabolic diseases.

We described a murine model in which exposure to a low-protein diet during gestation has critical effects on the development of  $\beta$  cells in early life and on metabolism in adult life. Although not unprecedented, we did not observe a reduction in maternal body weight during pregnancy or in offspring body weight at birth, and we did not observe catch-up growth (20, 31). Similar to findings from earlier studies, we have shown reduction in  $\beta$  cell fraction at birth and glucose intolerance despite enhanced insulin sensitivity in early adult life (11, 13, 20, 32–35). The reduction in  $\beta$  cell fraction at birth normalizes to control levels at 3 months of age and likely has no role in the glucose intolerance observed in adult LP0.5 mice. Rather, the results of the metabolic studies in vivo and in vitro revealed that the alterations in glucose homeostasis are a result of an insulin secretory defect in LP0.5  $\beta$  cells. Interestingly, LP0.5 mice do not develop diabetes despite a significant defect in insulin secretion because they are more insulin sensitive, as previously shown in other studies (33, 35). The increase in insulin sensitivity could result from an enhanced number of insulin receptors in the livers of LP0.5 mice, as previously reported (36).

In the present study, we determined that LP0.5 islets exhibit normal levels of intracellular calcium and the defect observed following KCl stimulations indicates that LP0.5  $\beta$  cells exhibit defects in insulin secretion that are distal to calcium influx. Our results are consistent with the concept that not only defects in proinsulin synthesis but also an insulin secretory defect from the islets contribute to a suboptimal insulin secretion in these mice. Reduced insulin content in LP0.5  $\beta$  cells has also been observed in studies in sheep and rats (11, 37). Downregulation of *Pdx1* protein levels and reduced ERK1/2 signaling could explain in part the reduction in *Ins2* transcription and insulin content in LP0.5  $\beta$  cells (10, 38, 39). Because two-thirds of insulin protein is derived from the conserved *Ins2* gene rodents (40), these data are not unexpected. It is also likely that the reduction of mTOR levels could also contribute to the insulin secretory defect in LP0.5  $\beta$  cells by altering the activity of mTORC1 and mTORC2. The importance of mTORC1 signaling for insulin secretion has been demonstrated in mice with gain and loss of S6K function (41, 42). In addition, islets from LP0.5 mice exhibited lower levels of AKT phosphorylation at Ser473, a surrogate marker of mTORC2 (mTOR/riCTOR) activity. The importance of mTORC2 for insulin content and insulin secretion has been established in mice with conditional ablation of rictor (43). Future studies could be designed to examine how mTORC2 regulates signaling and distal events (i.e., reorganization/remodeling of filamentous actin) responsible for vesicle trafficking and exocytosis (44, 45).

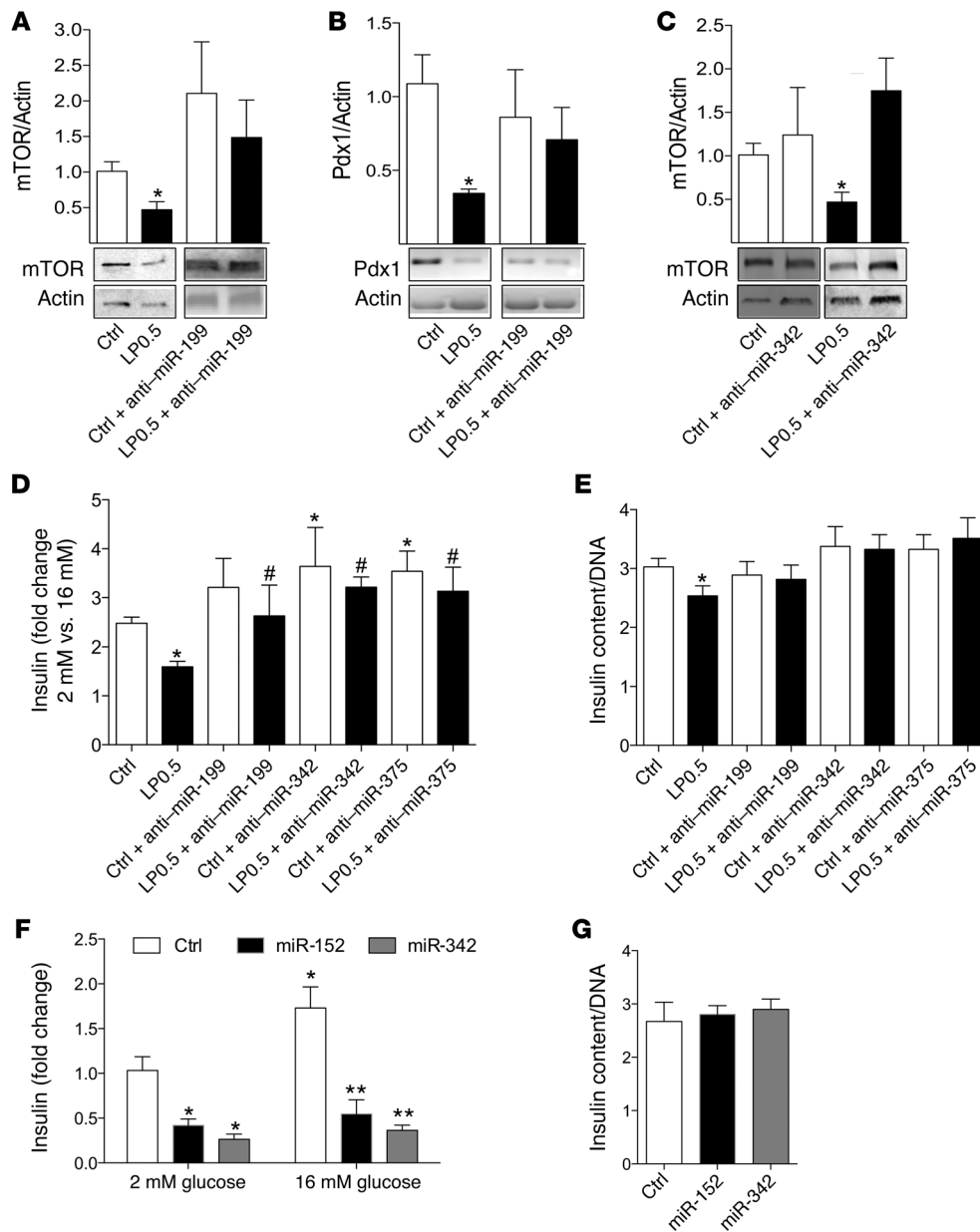


**Figure 8. miR-199a-3p and -342 regulate mTOR protein levels and insulin secretion in  $\beta$  cells.** (A and B) mTOR (A) and Pdx1 (B) protein levels in dispersed islet cells treated with or without anti-miR-199a-3p (199). (C) mTOR protein levels in dispersed islet cells treated with or without anti-miR-342. (D and E) Insulin secretion (D) and insulin content (E) in dispersed  $\beta$  cells from 12-week-old male LP0.5 and control islets treated with or without anti-miR-199, -342, or -375. (F and G) Insulin secretion (F) and insulin content normalized to DNA (ng/ml) (G) in  $\beta$  cells from 12-week-old male control islets treated with or without miR-152 and -342 mimics.  $n = 3-6$ . \* $P < 0.05$  vs. Ctrl, \* $P < 0.05$  vs. LP0.5, \*\* $P < 0.05$  vs. Ctrl in high glucose (16 mM glucose).

We, and others, have established that mTOR signaling plays a major role in regulating  $\beta$  cell mass and function (15, 17, 46, 47). In the present study, we have identified for the first time that downregulation of mTOR protein levels in LP0.5 islets is one of the mechanisms involved in the programming of  $\beta$  cells. Our data reveal that exposure to LP0.5 is sufficient to permanently reduce islet mTOR protein levels. The reduction in mTOR expression was not sufficient to decrease total protein synthesis, suggesting that this mechanism is unlikely to play a role in the LP0.5 phenotype (data not shown). This is not surprising, as total protein synthesis in islets from mice lacking 1 allele of mTOR (*Pdx1-Cre mTOR<sup>f/f</sup>* mice) is comparable to that of control mice (*mTOR<sup>f/f</sup>*) (E.U. Alejandro et al., unpublished data). The reduction in mTOR level, however, was associated with reduced  $\beta$  cell fraction at birth, suggesting that  $\beta$  cell expansion is sensitive to mTOR levels. However, the defect in mTOR

expression was not sufficient to alter the significant  $\beta$  cell mass expansion observed during the first 4 weeks of life, as  $\beta$  cell mass was normalized in adult mice (48-50).

A major finding of the current study is that a significant number of miRs induced in LP0.5 islets (miR-199a-3p, -342, and -7a) target different components of mTOR signaling. mTOR protein was reduced in adult LP0.5 islets due to upregulation of novel miRs. We found that LP0.5 exposure during pregnancy induced upregulation of miR-199a-3p in adult LP0.5 islets. This miR has been shown to directly bind to mTOR 3'UTR and affect mTOR protein translation in 3 models of hepatocarcinoma-derived cell lines (24), which is consistent with the normalization of mTOR levels in LP0.5 islets after transfection of anti-miR-199a-3p. We also demonstrated a novel role of miR-342 on regulation of mTOR protein, as blocking miR-342 normalized mTOR protein expressions in adult LP0.5 islets. Moreover, blockade of miR-199a-3p

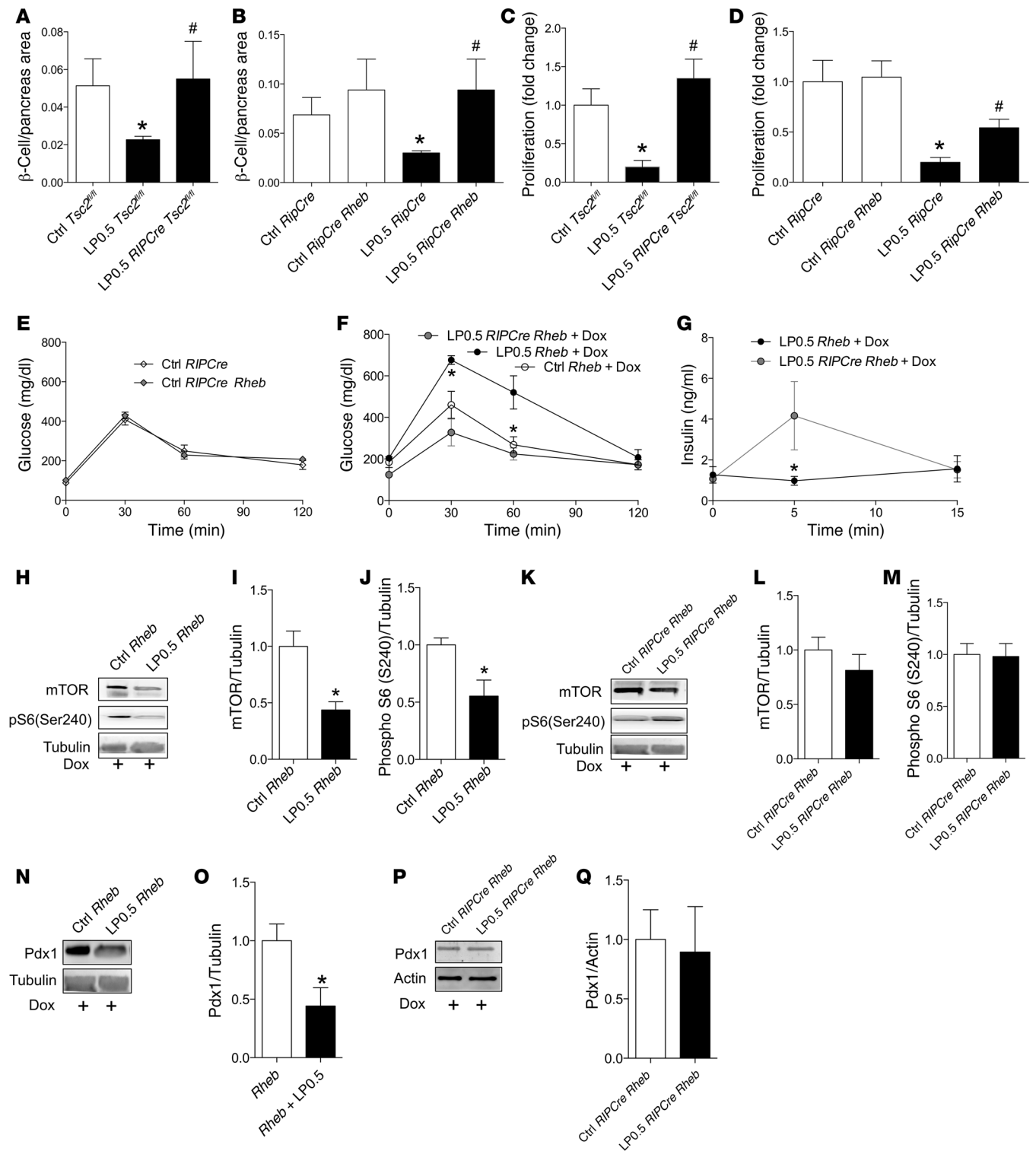


**Figure 9. Transient activation of mTORC1 in  $\beta$  cells during development rescues neonatal  $\beta$  cell fraction, glucose intolerance, and insulin secretion dysfunction in LP0.5 mice.** (A and B) Newborn  $\beta$  cell/pancreas area in *Tsc2<sup>fl/fl</sup>*, *RIPCre Tsc2<sup>fl/fl</sup>*, *RIPCre*, or *RIPCre Rheb* Ctrl or LP0.5 mice ( $n = 3-5$ ). (C and D)  $\beta$  Cell proliferation in *Tsc2<sup>fl/fl</sup>*, *RIPCre Tsc2<sup>fl/fl</sup>*, *RIPCre*, or *RIPCre Rheb* Ctrl or LP0.5 mice ( $n = 3-5$ ). (E) Intraperitoneal glucose test in 12-week old male *RIPCre Rheb* and wild-type *RIPCre* mice without Dox ( $n = 6$ ). (F and G) Intraperitoneal glucose test and glucose-stimulated insulin secretion in *RIPCre Rheb* (LP0.5) and wild-type *Rheb* (LP0.5) mice exposed to Dox throughout life ( $n = 3$ ). (H-M) mTOR protein levels and phosphorylated S6 (Ser240) in islets from *Rheb* and *RIPCre Rheb* Ctrl or LP0.5 mice after exposure to Dox throughout life ( $n = 3$ ). (N-Q) Pdx1 protein levels in islets from *Rheb* and *RIPCre Rheb* Ctrl or LP0.5 mice with Dox after birth to death ( $n = 3-6$ ). \* $P < 0.05$  vs. Ctrl, # $P < 0.05$  vs. LP0.5.

and -342 not only resulted in increased mTOR protein expression but also improved insulin secretion (Figure 8, A–D), further providing evidence that mTOR signaling could play a role in the insulin secretory defect observed in LPO.5 islets (42, 43, 51). In contrast to mTOR, there are no putative target sites for miR-199a-3p, -152, and -342 on *Pdx1* or *Ins2* mRNA, and transfection of these miRs failed to alter *Pdx1* levels in INS1 cells, suggesting that *Pdx1* is not a direct target of these miRs (Supplemental Figure 8A). However, transfection of LPO.5 islets with anti-miR-199a-3p normalized mTOR and *Pdx1* protein levels between LPO.5 and control islets (Figure 8B). This suggests that miR-199a-3p indirectly regulates *Pdx1* by modulating pathways that restore *Pdx1* at the transcriptional, posttranscriptional, or protein stability level and is perhaps mediated by modulation of mTOR activity. Indeed, activation of mTORC1 during pregnancy restored mTOR levels and signaling, and this was associated with normalization of *Pdx1* levels (Figure 9, H–Q). Further evidence for the regulation of *Pdx1* by mTOR comes from mice overexpressing a kinase-dead mTOR in  $\beta$  cells. These mice exhibited decreased levels of *Pdx1* in islets (E.U. Alejandro et al., unpublished observations).

Alterations in other important targets of these miRs could also explain the abnormalities in insulin secretion induced by LPO.5. miR-7a, one of the most abundant miRs in adult islets, has been shown to target multiple proteins (p70S6K, eIF4E, Mknk1, and Mknk2) involved in the mTOR signaling pathway in  $\beta$  cells (22). Although miR-7a has been reported to have no effect on mTOR protein levels (22), it is possible that miR-7a could regulate insulin secretion by modulating S6K (42) and genes that regulate insulin granule exocytosis in  $\beta$  cells (52). Most recently, Latreille et al. elegantly showed that miR-7a controls  $\beta$  cell function in vivo by directly regulating genes that control late stages of insulin granule fusion with the plasma membrane (52), corroborating the insulin secretion dysfunction in LPO.5. Therefore, it is possible that LPO.5-induced miRs modulate insulin secretion by a combination of different mechanisms that include regulation of mTOR levels and signaling, insulin granule exocytosis, and insulin content.

The present study also revealed that a subset of novel miRs are involved in regulation of insulin secretion. In particular, inhibition of miR-199a-3p and -342 restored insulin secretion in adult LPO.5 islets. The alteration of insulin secretion by these miRs in LPO.5 islets could result from normalization of mTOR protein expression or from independent effects of these miRs on target proteins involved in insulin content and exocytosis. Normalization of insulin content in LPO.5 islets to control levels suggests that miR-199a-3p, -342, and -375 could also target insulin transcript stability or translation. Anti-miR-199a-3p also normalized *Pdx1* levels in LPO.5 islets, suggesting that this miR could indirectly regulate *Pdx1* by modulating the pathway that restores *Pdx1* at the transcriptional, posttranslational or protein stability level, and this could be a mechanism for restoration of insulin content by this miR. Overexpression of miR-342 and miR-152 (another novel miR enhanced in LPO.5 islets) blunted insulin secretion in islet cells, indicating novel roles for these miRs in insulin secretion. miR-152 is expressed in MIN6 mouse insulinoma cells (28) and validated targets in endometrial cancer cell lines, including rictor, an mTORC2-associated protein implicated to regulate both insulin content and insulin

secretion in vivo (26, 43). Potential targets of miR-152 and -342, including ribosomal protein S6, Ras GTPase-activating protein, profilin-2, syntaphilin, and syntaxin-binding protein 5, could alter insulin secretory functions identified using the miRGen database. In addition to miR-199a-3p and -342, blocking miR-375 was sufficient to restore insulin secretion in LPO.5 islets. Interestingly, miR-375 inhibits insulin secretion at a distal stage independent of calcium signaling (28). Therefore, miR-372 affects events that occur after induction of calcium signaling (i.e., insulin granule fusion to the plasma membrane) is sufficient to ameliorate insulin secretion dysfunction in LPO.5 islets. In summary, we have identified a subset of islet miRs that are regulated permanently by exposure to protein restriction during fetal life. How LPO.5 controls expression of the miRs is an open question that is worth pursuing in the future. To gain insight into the upstream factors that could regulate the expression of these miRs, we have looked at the promoter elements of the different miRs and found that the majority of these miRs are regulated by methylation of the promoters (miR-342, -152, and -199a-3p-a1). Interestingly, miR-199a-3p-a2 and -7a contain E-boxes, suggesting that Ngn3 and NeuroD/ $\beta$ 2 could be implicated (53, 54). Taken together, we conclude that this group of miRs could alter insulin secretion by several mechanisms, including insulin biosynthesis and distal events that involve the secretory machinery; however, the mechanisms of upstream factors that regulate these miRs are still unclear.

Our studies using genetic models provide further evidence that alteration of mTORC1 signaling in  $\beta$  cells during developmental stages plays a central role in the metabolic programming induced by LPO.5. Gain of mTORC1 function by conditional deletion of TSC2 or Rheb overexpression in  $\beta$  cells during development was sufficient to rescue the neonatal  $\beta$  cell fraction defect in LPO.5 mice. Together with the reduced phosphorylated S6 staining in neonatal  $\beta$  cells, these results suggest that the effects of protein restriction on  $\beta$  cell growth during development are mediated in part by mTORC1 signaling. More importantly, transient gain of mTORC1 function by inducible Rheb expression during the last week of fetal developmental was sufficient to partly restore mTOR and *Pdx1* protein levels, reversing the insulin secretory defect and glucose intolerance in adult LPO.5 mice. The beneficial effect of Rheb overexpression during fetal stages on glucose tolerance in adult LPO.5 mice was not explained by changes in  $\beta$  cell mass, suggesting that mTORC1 induction during embryonic stages positively affects insulin secretion later in life. Although the mechanisms responsible for this are not completely understood, the current experiments suggest that an increase in mTORC1 during gestation restores mTORC1 activity and insulin secretion in LPO.5 mice by mechanisms that are independent of miR expression. Future experiments could test whether mTOR signaling and miRs act on common pathways to regulate insulin granule exocytosis. Interestingly, constitutive  $\beta$  cell Rheb expression during development does not significantly enhance neonatal  $\beta$  cell/pancreas area in mice exposed to Ctrl. Moreover, these mice do not show improvement in glucose tolerance at 3 months of age, suggesting that increased mTORC1 signaling has no additional effects in control or basal conditions. As such, in conditions such as low-protein diet, in which there is reduced or less than optimal mTORC1 sig-

naling, additional activation of the mTORC1 pathway can have beneficial effects. This can be explained in part by lower expression levels of Rheb obtained in heterozygous versus homozygous Rheb mice. It is possible that this phenotype could be different in homozygous Rheb-inducible transgenic mice, and experiments investigating this are currently underway.

In summary, this study highlights the importance of the nutrient environment for developing  $\beta$  cells and provides strong evidence that mTOR is a key player in regulating  $\beta$  cell programming by low-protein diet. We have identified that mTOR protein expression is regulated by multiple miRs sensitive to nutrients. Furthermore, we generated multiple murine models that were genetically capable of inducing mTORC1 specifically in  $\beta$  cells during the last week of gestation of LPO.5 offspring and demonstrated that these mice are resistant to the neonatal  $\beta$  cell mass defect and glucose intolerance and restored insulin secretion dysfunction caused by low-protein programming in adult mice. Insights gained from this study may help inform the design of treatments and prevention of T2D in individuals with IUGR.

## Methods

**Low-protein C57BL/6 strain mouse model.** Virgin C57BL/6 females and males at 2 months of age were purchased from The Jackson Laboratories and allowed to adapt to Ctrl (D02041001B, Research Diets Inc.) for 4 weeks (Figure 1A). After acclimation to the Ctrl, females and males were housed together for up to 3 days. Females were checked daily for vaginal plugs. Upon detection of a vaginal plug (designated E0.5), females were single housed and fed either low-protein (9%, D02041002, Research Diets Inc.) or control (23%, D02041001B) chow until delivery (Figure 1A). Both diets are isocaloric but differ in the amount of protein in the form of casein (complete diet composition is shown on Supplemental Table 1). Pregnant dams delivered spontaneously on gestational day 19. Females were switched to normal chow immediately after delivery (23%, D02041001B).

**Generation of conditional *RIPCre Tsc2<sup>fl/fl</sup>* and *RIPCre Rheb* mice.** To induce mTORC1 signaling in  $\beta$  cells we generated 2 models: (a) conditional deletion of TSC2, a negative regulator of mTORC1, and (b)  $\beta$  cell-specific overexpression of Rheb, a positive regulator of mTORC1. First, we crossed female *Tsc2<sup>fl/fl</sup>* mice (15) with male mice harboring both *Tsc2<sup>fl/fl</sup>* and Cre recombinase (55) under the rat insulin 2 promoter (*RIPCre Tsc2<sup>fl/fl</sup>*) (15). Second, we crossed female *RIPCre Rheb* (*Rheb<sup>tTA</sup>*) mice with male *RIPCre* mice. Briefly, *RIPCre Rheb* mice were generated by a knockin strategy using a backbone knockin ROSA-26-tetracycline-regulated transcriptional activator (tTA) as previously described (56). The expression of the Rheb transgene and an internal ribosome entry site controlling expression of EGFP is Dox dependent. The crosses were set up in a manner such that embryos with gain of mTORC1 function (*RIPCre Tsc2<sup>fl/fl</sup>* or *RIPCre Rheb*) and wild-type (*Tsc2<sup>fl/fl</sup>*, *Rheb*, or *RIPCre*) were littermate offspring from dams (*Tsc2<sup>fl/fl</sup>* or *Rheb*) exposed to LPO.5 or Ctrl throughout pregnancy. The rescue model was set up similarly as the C57BL/6 strain mouse model above. However, after delivery, LPO.5 and control dams and offspring were introduced to Ctrl containing Dox (23%, 200 mg Dox per kg, D11071101, Research Diets Inc.). Mice included in experiments were on a mixed 129 and C57BL/6 background; *Tsc2<sup>fl/fl</sup>* and *RIPCre Tsc2<sup>fl/fl</sup>* or *Rheb* and *RIPCre Rheb* littermates were on comparable mixed backgrounds.

**Pancreas section collection.** Newborn pancreata from each group (C57BL/6 mice and mice with *Tsc2<sup>fl/fl</sup>*, *RIPCre Tsc2<sup>fl/fl</sup>*, *Rheb*, and *RIPCre Rheb* genotypes) exposed to LPO.5 or Ctrl were harvested on P1. Adult pancreata were harvested on day 90 in C57BL/6 LPO.5 and control mice. Pancreata were fixed in 3.7% formalin in PBS for 6 hours (newborn pancreas) or overnight (adult pancreas).

**Primary mouse islet isolation.** Islets were isolated by collagenase digestion (57). The pancreas was perfused via the common duct with 1 mg/ml collagenase XI (Sigma-Aldrich) in HBSS (Life Technologies). Pancreatic digestion was carried out at 37°C for 15 minutes, after which cold HBSS with 2.5% FBS (Life Technologies) was added. The suspension was centrifuged at 330 g for 30 seconds; washed 3 times with HBSS with 2.5% FBS; resuspended in RPMI 1640 with 5 mM glucose, 10% FBS, 100 IU/ml penicillin, and 100 g/ml streptomycin; and poured onto a 70- $\mu$ m cell strainer (BD Falcon, BD Biosciences). Islets were rinsed and handpicked. Islets were allowed to recover overnight before experiments were carried out.

**Primary mouse islet insulin secretion analysis in vitro.** Isolated islets were cultured overnight with regular RPMI 1640 media containing 5 mM glucose and 10% FBS. The following day, islet cells were washed twice with PBS and cultured in serum-free media and 2 mM glucose for 1 hour before placement in 2 mM or 16 mM glucose for 15 minutes. To assess maximum capacity for insulin secretion, we used 30 mM KCl for 10 minutes. Insulin secretion levels were measured using either radioimmunoassay (Rat Insulin RIA, Millipore) or ELISA (Mouse-Insulin UltraSensitive, ELISA, ALPCO Immunoassays).

**Insulin secretion analysis in dispersed islet cells in vitro.** Approximately 750 to 1,000 islets from either Ctrl or LPO.5 mice were isolated and allowed to recover overnight in RPMI 1640 media with 10% FBS and 5 mM glucose. Islet dispersion was carried out by 4 consecutive washes with Ca<sup>2+</sup>/Mg<sup>2+</sup>-free MEM, followed by a gentle repetitive pipetting with trypsin-EDTA solution diluted 1:9 in MEM. Cells were washed 4 times with Ca<sup>2+</sup>/Mg<sup>2+</sup>-free MEM and seeded onto 9 wells of a 24-well plate with MEM for 3 hours. Media was then replaced with OPT-MEM containing Lipofectamine 2000 complexes with control or individual MiRVana miR inhibitors or a cocktail of MiRVana miR inhibitors of miR-199, -342, and -375 or mimics for miR-152 and -342 (30 nmol/l for each miR). Twelve hours after transfection, media were removed and replaced with RPMI 1640 media with 5 mM glucose and 10% FBS. Cells were allowed to recover for an additional 24 hours before glucose-stimulated insulin secretion, which required a 2-hour preincubation with a Krebs-Ringer buffer containing 129 mM NaCl, 5 mM NaHCO<sub>3</sub>, 4.8 mM KCl, 2.5 mM CaCl<sub>2</sub>, 1.2 mM MgSO<sub>4</sub>, 1.2 mM KH<sub>2</sub>PO<sub>4</sub>, 10 mM HEPES, 2 mM glucose, and 2 g/l essentially free fatty acid BSA (Sigma-Aldrich). Transfected cells were then exposed in Krebs-Ringer buffer with 2 mM glucose for 30 minutes before exposure to 25 mM glucose for another 30 minutes. Collected media samples were spun down for 5 minutes at 500 g at 4°C before storing at -80°C or prior to an insulin ELISA assay (ALPCO). Insulin content was analyzed from homogenized dispersed islet cells samples. Five independent cultures of triplicates were analyzed, and each experimental run was performed on a different day. All reagents used to this point were purchased from Life Technologies unless otherwise stated.

**Primary human islets.** Human islets provided by the Integrated Islet Distribution Program were dispersed and maintained in 5 mM glucose, 10% FBS RPMI, for 3 hours, followed by transfection with 30

nmol/l anti-miR-199 or control oligonucleotides by Lipofectamine 2000 (Life Technologies) for 12 hours. 24 hours after transfection, glucose-stimulated insulin secretion was performed, and then cells were harvested for Western blotting. Human islets were obtained from 4 male normoglycemic donors (2 African-American men and 2 men of mixed European descent, with an average BMI of 31; ages: 24, 25, 52, and 57 years).

**Immunostaining and islet morphology analysis.** Formalin-fixed pancreatic tissues were embedded in paraffin using standard techniques. 5- $\mu$ m sections were deparaffinized, rehydrated, and incubated with blocking solution as previously described (57). Sections were incubated overnight at 4°C with antibodies against insulin (anti-guinea pig, Dako), Ki67 (Vector Laboratories), and phosphorylated S6 (Ser240, Ser235, Cell Signaling), followed by secondary antibodies conjugated to FITC or Cy3 (Jackson ImmunoResearch). DAPI-containing mounting media (Vector Laboratories) was added to coverslips. Total pancreas and insulin-positive cell areas from 5 insulin-stained sections (5  $\mu$ m) separated by 50  $\mu$ m (newborn pancreas) or 200  $\mu$ m (adult pancreas) were measured by using Image Pro Software (Media Cybernetics).  $\beta$  Cell fraction or mass (average  $\beta$  cell fraction multiplied by pancreas weight) assessment was performed using Objective Imaging's Surveyor automated scanning with a Leica fluorescent microscope (Leica Microsystems). Proliferating cells were identified by costaining for monoclonal rabbit anti-Ki67 and insulin. At least 1,000–3,000 stained cells were counted from each treatment and  $n = 4$ –5 per group were analyzed.

**Protein and RNA isolation.** Protein and RNA samples were prepared from 3 to 4 islet preparations, acini, and liver samples from each treatment group. Samples were quickly washed with PBS prior to incubation in lysis buffer (Cell Signaling) or with Trizol (Sigma-Aldrich). Samples were flash frozen with liquid nitrogen and then kept at –80°C prior to homogenization. RNA for gene expression analysis was isolated using Trizol with columns (Qiagen). RNA for miR analysis was isolated using RNeasy and the RNeasy MicroRNA Kit (Life Technologies).

**Quantitative real-time PCR for gene and miR expression.** Total RNA for gene expression analysis was isolated using RNeasy (Qiagen). cDNA synthesis was performed using random hexamers and was reverse transcribed using SuperScript II (Life Technologies) according to the manufacturer's protocol. Real-time PCR was performed on an ABI 7000 sequence detection system using SYBR Green (Applied Biosystems). Primers were purchased from Applied Biosystems. Primers used are listed in Supplemental Table 2. RNA for miR analysis was isolated using RNeasy and the RNeasy MicroRNA Kit (Life Technologies). For mature miR transcript expression, we used Taqman MicroArray Assays (Life Technologies).

**OpenArray miR arrays.** Each TaqMan OpenArray MicroRNA Panel contains 754 well-characterized miR sequences from the Sanger miR-Base v14. All 754 assays have been functionally validated with miR artificial templates. Full-service processing by the University of Michigan Microarray Core Facility included assessment of RNA quality by an Agilent Bioanalyzer, probe labeling from total RNA submitted, hybridization, scanning, and data analysis. Islets were harvested from LPO.5 and Ctrl mice 2- to 3-months of age, and RNA was isolated by the RNeasy MicroRNA Kit for OpenArray microarray ( $n = 5$ ). The microarray data have been deposited in a MIAME-compliant public database through NCBI (GEO accession no. GSE59279).

**Protein quantifications.** Immunoblotting was performed as previously described (58). Briefly, islet cells were washed after treatment with PBS before adding cell lysis buffer (Cell Signaling) with protease inhibitor cocktail and phosphoStop tablets (Roche Applied Science). Primary antibodies against mTOR, phosphorylated S6 (Ser240 and 235), AKT (Ser473), and total AKT were from Cell Signaling. An antibody against mouse  $\beta$ -actin was from Sigma-Aldrich. Pdx1 and MafA antibodies were from Millipore and Novus Biologicals, respectively. Densitometry analysis was performed using ImageJ (NIH).

**Measurements of intracellular  $Ca^{2+}$ .** Islets were preloaded with 2.5  $\mu$ M Fura2-AM (Molecular Probes) in 0.1% DMSO for 30 minutes at 37°C and washed for 10 minutes before recording. The recording solution contained 145 mM NaCl, 5 mM KCl, 1.2 mM  $MgCl_2$ , 2.6 mM  $CaCl_2$ , 10 mM HEPES, and glucose as indicated (pH 7.4). Imaging parameters were identical to those in Merrins et al. (59), and  $Ca^{2+}$  is reported as the emission ratio R340/380.

**Glucose and insulin tolerance tests.** Glucose and insulin tolerance tests were performed by intraperitoneal delivery of 2 g/kg glucose or 0.75 unit/kg insulin (Novolin, Novo Nordisk Inc.) to mice after 15 hours or 6 hours of fasting respectively. Blood glucose was monitored for 2 hours after glucose or insulin delivery. Fasting glucose and insulin were measured by obtaining blood from tail veins after overnight fasting. Glucose was measured using the AccuChek II glucometer (Abbott). Plasma insulin levels were measured using the Mouse Insulin ELISA Kit (ALPCO).

**Measurement of islet insulin content.** Islet insulin content was measured by placing 10 size-matched islets into a 1.5-ml tube containing 100  $\mu$ l lysis buffer (Cell Signaling). Samples were diluted 1:1,000 in Krebs-Ringer buffer, and insulin content was measured with the Mouse Insulin ELISA Kit (ALPCO). Insulin levels were corrected to total DNA measured by a Qubit Fluorometer (Life Technologies).

**Metabolic labeling and immunoprecipitation.** Metabolic labeling and immunoprecipitation were performed as previously described (60). Briefly, isolated adult LPO.5 and control islets were incubated in RPMI containing 5.5 mM glucose and 10% FBS overnight before being pulse labeled with  $^{35}S$ -labeled amino acids for 10 minutes and chased for 60 and 150 minutes as indicated. Fifteen islets per animal were used for each sample, and 3 independent experiments were performed from 3 different cohorts of mice (3 mice used per experiment). Islets cells and chase media collected were immunoprecipitated with a polyclonal anti-insulin antibody that recognizes all insulin forms. Newly synthesized proinsulin and processed insulin were analyzed using Nu-Page gel under reducing conditions.

**Statistics.** Data are presented as mean  $\pm$  SEM. Data were analyzed by a 2-tailed Student's  $t$  test or by a nonparametric  $U$  test with Mann-Whitney analysis using GraphPad Prism version 6 (GraphPad Software), where appropriate. Results were considered statistically significant when the  $P$  value was less than 0.05.

**Study approval.** All animal care and procedures were in accordance with active animal study protocols at the University of Michigan. All procedures related to human T2D islets were approved by ethics committees through the Integrated Islet Distribution Program. Informed consent was obtained from all subjects.

## Acknowledgments

This work was supported by NIH grants R01DK073716 and 2R01DK073716 and a Career Development Award from the Amer-

ican Diabetes Association (to E. Bernal-Mizrachi). E.U. Alejandro was supported by an NIH training grant (2T32DK071212-06) and a postdoctoral fellowship from the Hartwell Foundation. Work in the Satin lab was supported by NIH grant R01-DK-46409. Work in the Liu lab was supported by NIH grant R01-DK088856. The authors acknowledge support from the Morphology and Image Analysis Core, Metabolomics Core, and Phenotyping Core from the Michigan Diabetes Research Center (P30 DK020572). We thank Joshua Scheys for discussion and Corentin Cras-Méneur

and Lynda Elghazi for discussion and technical assistance with newborn pancreas dissection. We acknowledge Michelle Smith for technical assistance with animal husbandry.

Address correspondence to: Ernesto Bernal-Mizrachi, Department of Internal Medicine, Division of Metabolism, Endocrinology and Diabetes, 1000 Wall Street, 5122, University of Michigan, Ann Arbor, Michigan 48109-0678, USA. Phone: 734.615.0262; E-mail: ebernal@umich.edu.

- Lango H, et al. Assessing the combined impact of 18 common genetic variants of modest effect sizes on type 2 diabetes risk. *Diabetes*. 2008;57(11):3129–3135.
- Morris AP, et al. Large-scale association analysis provides insights into the genetic architecture and pathophysiology of type 2 diabetes. *Nat Genet*. 2012;44(9):981–990.
- Sandovici I, Hammerle CM, Ozanne SE, Constância M. Developmental and environmental epigenetic programming of the endocrine pancreas: consequences for type 2 diabetes. *Cell Mol Life Sci*. 2013;70(9):1575–1595.
- Hales CN, Barker DJ. Type 2 (non-insulin-dependent) diabetes mellitus: the thrifty phenotype hypothesis. *Diabetologia*. 1992;35(7):595–601.
- Fernandez-Twinn DS, Ozanne SE. Early life nutrition and metabolic programming. *Ann N Y Acad Sci*. 2010;1212:78–96.
- Snoeck A, Remacle C, Reusens B, Hoet JJ. Effect of a low protein diet during pregnancy on the fetal rat endocrine pancreas. *Biol Neonate*. 1990;57(2):107–118.
- Hoet JJ, Snoeck A, Reusens-Billen B, Remacle C, Hoet JJ. Islet function in offspring of mothers on low-protein diet during gestation. *Diabetes*. 1991;40(suppl 2):115–120.
- Lucas A. Programming by early nutrition in man. *Ciba Found Symp*. 1991;156:38–50; discussion 50–55.
- Sandovici I, et al. Maternal diet and aging alter the epigenetic control of a promoter-enhancer interaction at the Hnf4a gene in rat pancreatic islets. *Proc Natl Acad Sci U S A*. 2011;108(13):5449–5454.
- Park JH, Stoffers DA, Nicholls RD, Simmons RA. Development of type 2 diabetes following intrauterine growth retardation in rats is associated with progressive epigenetic silencing of Pdx1. *J Clin Invest*. 2008;118(6):2316–2324.
- Petrik J, et al. A low protein diet alters the balance of islet cell replication and apoptosis in the fetal and neonatal rat and is associated with a reduced pancreatic expression of insulin-like growth factor-II. *Endocrinology*. 1999;140(10):4861–4873.
- Roos S, Jansson N, Palmberg I, Säljö K, Powell TL, Jansson T. Mammalian target of rapamycin in the human placenta regulates leucine transport and is down-regulated in restricted fetal growth. *J Physiol*. 2007;582(pt 1):449–459.
- Bhasin KK, van Nas A, Martin LJ, Davis RC, Devaskar SU, Lusis AJ. Maternal low-protein diet or hypercholesterolemia reduces circulating essential amino acids and leads to intrauterine growth restriction. *Diabetes*. 2009;58(3):559–566.
- Teodoro GF, et al. Leucine is essential for attenuating fetal growth restriction caused by a protein-restricted diet in rats. *J Nutr*. 2012;142(5):924–930.
- Rachdi L, et al. Disruption of Tsc2 in pancreatic  $\beta$  cells induces  $\beta$  cell mass expansion and improved glucose tolerance in a TORC1-dependent manner. *Proc Natl Acad Sci U S A*. 2008;105(27):9250–9255.
- Mori H, et al. Critical role for hypothalamic mTOR activity in energy balance. *Cell Metab*. 2009;9(4):362–374.
- Blandino-Rosano M, et al. mTORC1 signaling and regulation of pancreatic  $\beta$ -cell mass. *Cell Cycle*. 2012;11(10):1892–1902.
- Xu G, Kwon G, Cruz WS, Marshall CA, McDaniel ML. Metabolic regulation by leucine of translation initiation through the mTOR-signaling pathway by pancreatic  $\beta$ -cells. *Diabetes*. 2001;50(2):353–360.
- Rachdi L, Aiello V, Duvillie B, Scharfmann R. L-leucine alters pancreatic  $\beta$ -cell differentiation and function via the mTOR signaling pathway. *Diabetes*. 2012;61(2):409–417.
- Cox AR, Gottheil SK, Arany EJ, Hill DJ. The effects of low protein during gestation on mouse pancreatic development and  $\beta$  cell regeneration. *Pediatr Res*. 2011;68(1):16–22.
- Gu C, et al. Pancreatic  $\beta$  cells require NeuroD to achieve and maintain functional maturity. *Cell Metab*. 2010;11(4):298–310.
- Wang Y, Liu J, Liu C, Naji A, Stoffers DA. MicroRNA-7 regulates the mTOR pathway and proliferation in adult pancreatic  $\beta$ -cells. *Diabetes*. 2013;62(3):887–895.
- Sun D, et al. miR-99 family of MicroRNAs suppresses the expression of prostate-specific antigen and prostate cancer cell proliferation. *Cancer Res*. 2011;71(4):1313–1324.
- Fornari F, et al. MiR-199a-3p regulates mTOR and c-Met to influence the doxorubicin sensitivity of human hepatocarcinoma cells. *Cancer Res*. 2010;70(12):5184–5193.
- Wu D, Huang HJ, He CN, Wang KY. MicroRNA-199a-3p regulates endometrial cancer cell proliferation by targeting mammalian target of rapamycin (mTOR). *Int J Gynecol Cancer*. 2013;23(7):1191–1197.
- Tsuruta T, et al. miR-152 is a tumor suppressor microRNA that is silenced by DNA hypermethylation in endometrial cancer. *Cancer Res*. 2011;71(20):6450–6462.
- Megraw M, Sethupathy P, Corda B, Hatzigeorgiou AG. miRGen: a database for the study of animal microRNA genomic organization and function. *Nucleic Acids Res*. 2007;35(Database issue):D149–D155.
- Poy MN, et al. A pancreatic islet-specific microRNA regulates insulin secretion. *Nature*. 2004;432(7014):226–230.
- Pinney SE, Simmons RA. Metabolic programming, epigenetics, and gestational diabetes mellitus. *Curr Diab Rep*. 2012;12(1):67–74.
- Jimenez-Chillaron JC, et al.  $\beta$ -Cell secretory dysfunction in the pathogenesis of low birth weight-associated diabetes: a murine model. *Diabetes*. 2005;54(3):702–711.
- Heywood WE, Mian N, Milla PJ, Lindley KJ. Programming of defective rat pancreatic  $\beta$ -cell function in offspring from mothers fed a low-protein diet during gestation and the suckling periods. *Clin Sci (Lond)*. 2004;107(1):37–45.
- Dumortier O, Blondeau B, Duvillie B, Reusens B, Bréant B, Remacle C. Different mechanisms operating during different critical time-windows reduce rat fetal beta cell mass due to a maternal low-protein or low-energy diet. *Diabetologia*. 2007;50(12):2495–2503.
- Ozanne SE, Wang CL, Coleman N, Smith GD. Altered muscle insulin sensitivity in the male offspring of protein-malnourished rats. *Am J Physiol*. 1996;271(6):E1128–E1134.
- Lim JS, Lee JA, Hwang JS, Shin CH, Yang SW. Non-catch-up growth in intrauterine growth-retarded rats showed glucose intolerance and increased expression of PDX-1 mRNA. *Pediatr Int*. 2011;53(2):181–186.
- Gosby AK, Maloney CA, Caterson ID. Elevated insulin sensitivity in low-protein offspring rats is prevented by a high-fat diet and is associated with visceral fat. *Obesity (Silver Spring)*. 2010;18(8):1593–1600.
- Ozanne SE, Smith GD, Tikepae J, Hales CN. Altered regulation of hepatic glucose output in the male offspring of protein-malnourished rat dams. *Am J Physiol*. 1996;270(4):E559–E564.
- Cherif H, Reusens B, Dahri S, Remacle C. A protein-restricted diet during pregnancy alters in vitro insulin secretion from islets of fetal Wistar rats. *J Nutr*. 2001;131(5):1555–1559.
- Arantes VC, et al. Expression of PDX-1 is reduced in pancreatic islets from pups of rat dams fed a low protein diet during gestation and lactation. *J Nutr*. 2002;132(10):3030–3035.
- Khoo S, Griffen SC, Xia Y, Baer RJ, German MS, Cobb MH. Regulation of insulin gene transcription by ERK1 and ERK2 in pancreatic beta cells. *J Biol Chem*. 2003;278(35):32969–32977.
- Hay CW, Docherty K. Comparative analysis of insulin gene promoters: implications for diabetes research. *Diabetes*. 2006;55(12):3201–3213.

41. Pende M, et al. Hypoinsulinaemia, glucose intolerance and diminished  $\beta$ -cell size in S6K1-deficient mice. *Nature*. 2000;408(6815):994-997.
42. Elghazi L, et al. Decreased IRS signaling impairs  $\beta$ -cell cycle progression and survival in transgenic mice overexpressing S6K in  $\beta$ -cells. *Diabetes*. 2010;59(10):2390-2399.
43. Gu Y, Lindner J, Kumar A, Yuan W, Magnuson MA. Rictor/mTORC2 is essential for maintaining a balance between  $\beta$ -cell proliferation and cell size. *Diabetes*. 2011;60(3):827-837.
44. Kalwat MA, Thurmond DC. Signaling mechanisms of glucose-induced F-actin remodeling in pancreatic islet beta cells. *Exp Mol Med*. 2013;45:e37.
45. Huang W, et al. mTORC2 controls actin polymerization required for consolidation of long-term memory. *Nat Neurosci*. 2013;16(4):441-448.
46. Hamada S, et al. Upregulation of the mammalian target of rapamycin complex 1 pathway by Ras homolog enriched in brain in pancreatic  $\beta$ -cells leads to increased  $\beta$ -cell mass and prevention of hyperglycemia. *Diabetes*. 2009;58(6):1321-1332.
47. Mori H, Guan KL. Tissue-specific ablation of Tsc1 in pancreatic  $\beta$ -cells. *Methods Mol Biol*. 2012;821:407-419.
48. Bonner-Weir S. Life and death of the pancreatic beta cells. *Trends Endocrinol Metab*. 2000;11(9):375-378.
49. Bonner-Weir S. Islet growth and development in the adult. *J Mol Endocrinol*. 2000;24(3):297-302.
50. Finegood DT, Scaglia L, Bonner-Weir S. Dynamics of  $\beta$ -cell mass in the growing rat pancreas. Estimation with a simple mathematical model. *Diabetes*. 1995;44(3):249-256.
51. Park J, Um SH, Park J, D'Alessio D, Newgard CB, Kozma SC. Mammalian target of rapamycin is required for insulin secretion in pancreatic  $\beta$ -cells. *Diabetes*. 2011;60(suppl 1):A442-A521.
52. Latreille M, et al. MicroRNA-7a regulates pancreatic  $\beta$  cell function. *J Clin Invest*. 2014;124(6):2722-2735.
53. Sakurai K, et al. MicroRNAs miR-199a-5p and -3p target the Brm subunit of SWI/SNF to generate a double-negative feedback loop in a variety of human cancers. *Cancer Res*. 2011;71(5):1680-1689.
54. Kredon-Russo S, Ness A, Mandelbaum AD, Walker MD, Hornstein E. Regulation of pancreatic microRNA-7 expression. *Exp Diabetes Res*. 2012;2012:695214.
55. Herrera PL. Adult insulin- and glucagon-producing cells differentiate from two independent cell lineages. *Development*. 2000;127(11):2317-2322.
56. Banerjee S, Crouse NR, Emmett RJ, Gianino SM, Gutmann DH. Neurofibromatosis-1 regulates mTOR-mediated astrocyte growth and glioma formation in a TSC/Rheb-independent manner. *Proc Natl Acad Sci U S A*. 2011;108(38):15996-16001.
57. Bernal-Mizrachi E, Wen W, Stahlhut S, Welling CM, Permutt MA. Islet beta cell expression of constitutively active Akt1/PKB  $\alpha$  induces striking hypertrophy, hyperplasia, and hyperinsulinemia. *J Clin Invest*. 2001;108(11):1631-1638.
58. Bernal-Mizrachi E, et al. Defective insulin secretion and increased susceptibility to experimental diabetes are induced by reduced Akt activity in pancreatic islet  $\beta$  cells. *J Clin Invest*. 2004;114(7):928-936.
59. Merrins MJ, Van Dyke AR, Mapp AK, Rizzo MA, Satin LS. Direct measurements of oscillatory glycolysis in pancreatic islet  $\beta$ -cells using novel fluorescence resonance energy transfer (FRET) biosensors for pyruvate kinase M2 activity. *J Biol Chem*. 2013;288(46):33312-33322.
60. Liu M, Li Y, Cavener D, Arvan P. Proinsulin disulfide maturation and misfolding in the endoplasmic reticulum. *J Biol Chem*. 2005;280(14):13209-13212.